

FUNCTIONALIZED MEMBRANE WITH LIPID BILAYER FOR IMMOBILIZED ENZYMATIC SYSTEMS

Ph.D. THESIS

by

ANJU KUMARI



**DEPARTMENT OF BIOTECHNOLOGY
INDIAN INSTITUTE OF TECHNOLOGY ROORKEE
ROORKEE – 247 667 (INDIA)
MAY, 2018**

FUNCTIONALIZED MEMBRANE WITH LIPID BILAYER FOR IMMOBILIZED ENZYMATIC SYSTEMS

A THESIS

*Submitted in partial fulfilment of the
requirements for the award of the degree*

of

DOCTOR OF PHILOSOPHY

in

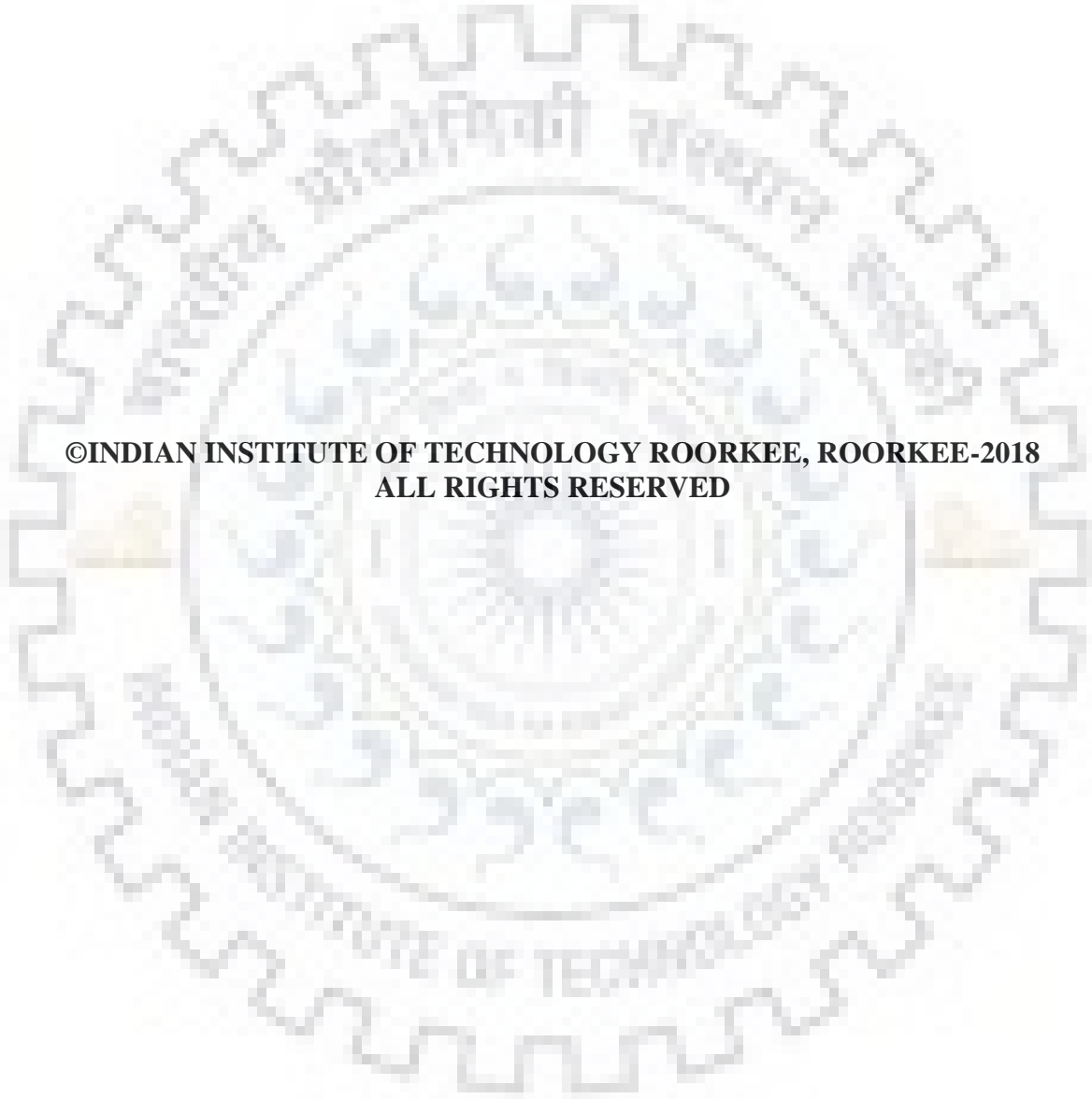
BIOTECHNOLOGY

by

ANJU KUMARI



DEPARTMENT OF BIOTECHNOLOGY
INDIAN INSTITUTE OF TECHNOLOGY ROORKEE
ROORKEE – 247 667 (INDIA)
MAY, 2018



**©INDIAN INSTITUTE OF TECHNOLOGY ROORKEE, ROORKEE-2018
ALL RIGHTS RESERVED**



INDIAN INSTITUTE OF TECHNOLOGY ROORKEE ROORKEE

CANDIDATE'S DECLARATION

I hereby certify that the work which is being presented in the thesis entitled "**FUNCTIONALIZED MEMBRANE WITH LIPID BILAYER FOR IMMOBILIZED ENZYMATIC SYSTEMS**" in partial fulfilment of the requirements for the award of the Degree of Doctor of Philosophy and submitted in the Department of Biotechnology of the Indian Institute of Technology Roorkee, Roorkee is an authentic record of my own work carried out during a period from July, 2014 to May, 2018 under the supervision of Dr. Saurav Datta, Assistant Professor, Department of Biotechnology, Indian Institute of Technology Roorkee, Roorkee.

The matter presented in this thesis has not been submitted by me for the award of any other degree of this or any other Institution.

(ANJU KUMARI)

This is to certify that the above statement made by the candidate is correct to the best of my knowledge.

(Saurav Datta)
Supervisor

Date: May 17, 2018

Abstract

Enzymes, immobilized within membrane pores, offer improved kinetics due to pressure driven convective flow. On the other hand, supported lipid bilayer (SLB), owing to its fluidity and native “cell-membrane” environment, facilitates the activity and stability of enzymes. In this study, the advantages of biomimetic characteristics of SLB and convective flow through microporous membrane were integrated within the same configuration. We report development of a novel biomimetic membrane by incorporating SLB within membrane pores using two different approaches – (i) direct deposition of lipid bilayer within bare membrane pores, and (ii) immobilization of a polymer cushion prior to lipid bilayer within membrane pores. As a model enzyme, glucose oxidase (GOx) was immobilized into the phospholipid bilayer network within the functionalized membrane pores. In-depth activity study was conducted with different GOx-functionalized membranes while monitoring the production of H₂O₂ by oxidation of glucose. In-depth activity study revealed that the biomimetic membrane containing polymer cushion supported SLB and operating under convective mode of flow exhibited benefits in terms of activity, stability and operating range of pH.

Therefore, we further extended our investigation and developed a novel bienzymatic system containing two enzymes, electrostatically co-immobilized, within phospholipid bilayer functionalized membrane pores. Glucose oxidase (GOx) and horseradish peroxidase (HRP) were used as model enzymes, and the two enzymes were immobilized using negative and positive charges, respectively. Again, two different approaches of direct deposition and polymer cushion supported lipid bilayer attachment within membrane pores were considered. Two different membrane configurations were also examined – (i) stack configuration, and (ii) co-immobilized configuration. Bienzymatic system containing polymer cushion supported lipid bilayer and present in co-immobilized configuration was superior to the other alternatives. The electrostatically immobilized bienzymatic system also exhibited improved stability and enabled a broader range of operating pH than the free enzymes. The major observation from GOx-HRP bienzymatic system was that two enzymes containing opposite charges can be electrostatically co-immobilized with zwitterionic DMPC molecules of SLB to give better activity and satisfying storage stability along with a broader range of operating pH. This finding was further extended to investigate the possibility of development of multienzymatic system.

A multienzymatic system containing glucoamylase (GA), GOx and HRP enzymes was developed by electrostatically incorporating all three enzymes within biomimetic membrane pores. CL membrane was selected to develop GA-GOx-HRP multienzymatic system. GOx-HRP enzymes were coimmobilized within a membrane, whereas GA was immobilized within a separate membrane. Both of these membranes were used in stack configuration, with the GA-membrane on top of the GOx-HRP membrane, for activity analysis of multienzymatic system. Activity analysis and storage stability were observed to be better for immobilized GA-GOx-HRP multienzymatic system than free enzymes due to the presence of the lipid bilayer functionalized membrane pores. Operating range of pH was also observed to be broader as observed earlier for immobilized GOx and GOx-HRP multienzymatic system.

The study was further extended for exploring the reusability of the membrane as well as the other functional components. The functionalized architecture was constructed based on electrostatic interactions, which facilitate reversible attachment-detachment sequence of the functional moieties. To demonstrate potential application, an enzyme, glucose oxidase (GOx), was electrostatically immobilized within the phospholipid bilayer functionalized membrane and enzymatic catalysis was conducted. Then, the enzyme was detached keeping the functional SLB backbone intact. Detachment of the enzyme without affecting the functional activity of SLB backbone permits attachment of fresh enzyme. In addition, reusability of the phospholipids is also of great importance as they have wide range of applications, but their usage is limited by higher cost. We have demonstrated detachment of the SLB from the membrane using a simple technique. Characterization of the detached phospholipid confirmed retention of the original structural and functional properties as exhibited before attachment.

Comparison of the results obtained in this study with other literature reported results establishes the benefits of the phospholipid bilayer functionalized biomimetic membrane operated under convective flow. To the best of our knowledge, this is the first study that investigates the advantages of incorporation of phospholipid bilayer within membrane pores for immobilized enzymatic catalysis and discusses the potential of reusability of the biomimetic membrane as well as the phospholipid. With further improvement in the strategy of functionalization and process optimization, this technique promises to deliver an efficient bioprocess for green synthesis of chemicals at larger scale.

Acknowledgement

I would like to express my immense gratitude to my supervisor **Dr. Saurav Datta**, for his continuous encouragement and motivation that has persuaded me to come up with completion of this project. I am grateful to my SRC members **Dr. Bijan Chaudhury**, **Dr. Raj Kumar Dutta** and **Dr. Kiran Ambatipudi** for their critical suggestions and assessments, which helped me all through to complete my tenure successfully.

I would like to express my gratitude to **Dr. A. K. Sharma**, Head of the Department, for providing all the infrastructural facilities in the department, which helped in completion of this endeavor. I also convey my regards to Dr. Sulakshana Mukherjee, Assistant Professor, Department of Biotechnology, Indian Institute of Technology Roorkee, for helpful discussion on NMR.

I sincerely and very dearly thank my lab mates **Mr. Ajay Kumar Sharma and Miss Ayushi Agarwal**, for all of their endless and unconditional support, encouragement and maintaining a much needed helpful work environment in lab. I also thank my colleague and lab mate **Mr. Bhanendra Singh** for helpful discussions.

I am also thankful to all the members of Biotechnology department, Chemistry department, Institute Instrumentation center, Chemical engineering department and Nanotechnology department who rendered their whole hearted support to all times for the completion of the project.

I would like to mention the unconditional and endless contributions of my family members, especially my father, **Mr. Sawaliya Tiwari**, who seeded the need and importance of higher studies in the very start of my educational venture. The support and encouragement of my husband, **Mr. Ashwani Pandey**, worked as boost towards the completion of my studies.

Finally, I convey my regards to Science and Engineering Research Board (SERB), Ministry of Human Resource and Development (MHRD), India for financially supporting this research through Ramanujan Fellowship Grant (Grant number: SB/S2/RJN-028/2014).

Table of Contents

Chapter 1. Introduction	1
Chapter 2. Literature review	4
Chapter 3. Objectives	13
Chapter 4. Materials & Methods	14
4.1. Equipments	14
4.2. Materials	14
4.2.1. Membrane	14
4.2.2. Chemicals	14
4.3. Analytical procedures	15
4.3.1. Quantification of Phospholipid	15
4.3.2. Quantification of enzymes	16
4.3.3. Quantification of glucose	17
4.3.4. Quantification of Hydrogen peroxide (H ₂ O ₂)	18
4.3.5. Quantification of ABTS	19
4.3.6. Activity analysis of immobilized GOx	20
4.3.7. Activity analysis of GOx-HRP bienzymatic system:	20
4.3.8. Activity analysis of GA-GOx-HRP multi-enzymatic system	21
4.4. Experimental Methods	21
4.4.1. Preparation of small unilamellar vesicles (SUVs) from DMPC	23
4.4.2. Functionalization of membrane pore with lipid bilayer	23
4.4.3. Immobilization of enzyme (GA or GOx or HRP) within functionalized membrane pores	26
4.4.4. Co-immobilization of GOx-HRP within biomimetic membrane	26
4.4.5. Effect of residence time (i.e., flow rate) on activity	26
4.4.6. Effect of pH on activity	27
4.4.7. Stability of the immobilized enzymatic system within functionalized membrane pores	27
4.4.8. Reusability of the functionalized membrane and SLB	28
Chapter 5. Results & Discussion	29
5.1. Characterization of small unilamellar vesicles (SUVs)	29

5.2. Functionalization of membranes and GOx immobilization	31
5.2.1. Functionalization of membrane with lipid bilayer	31
5.2.2. Immobilization of glucose oxidase (GOx)	33
5.2.3. Activity of immobilized GOx	34
5.2.4. Effect of operating conditions	37
5.2.4.1. Type of flow	37
5.2.4.2. Flow rate (residence time)	37
5.2.4.3. Effect of pH	39
5.2.5. Storage stability of immobilized GOx	40
5.3. Immobilized glucose oxidase (GOx)-horseradish peroxidase (HRP) bienzymatic System	42
5.3.1. Immobilization of GOx and HRP enzymes	42
5.3.2. Study of the activity of immobilized HRP enzyme	43
5.3.3. Activity of the immobilized GOx-HRP bienzymatic system	46
5.3.4. Operating range of pH for bienzymatic system	48
5.3.5. Storage stability of GOx-HRP bienzymatic system	50
5.4. Immobilization and activity of GA-GOx-HRP multienzymatic system	51
5.4.1. Immobilization of the enzymes	52
5.4.2. Activity of immobilized GA-GOx-HRP multienzymatic system	53
5.4.3. Operating range of pH for multienzymatic system	54
5.4.4. Storage stability of multienzymatic system	55
5.5. Reusability of the functionalized membrane and the phospholipid bilayer	56
5.5.1. Detachment of GOx – reusability of the SLB functionalized membrane	58
5.5.2. Detachment of SLB – reusability of the phospholipid	59
Chapter 6. Conclusion	61
Chapter 7. References	64

List of Tables

Table 5.1. Amount of lipid deposited and amount of GOx immobilized within the pores of bare nylon membrane (B), lipid deposited nylon membrane (L) and lipid deposited with cushion polymer on nylon membrane (CL). (Conditions: pore size of bare nylon membrane 0.2 μm , external membrane area 4.9 cm^2 and membrane thickness 160 μm) 32

Table 5.2 Amount of immobilized enzyme (nmol). B: Blank membrane, CL: Functionalized membrane with cushioned phospholipid bilayer, GOx and HRP enzymes were co-immobilized within same CL membrane 53



List of Figures

Figure 2.1. Mechanism of supported lipid bilayer (SLB) formation on a solid surface following Vesicle-Fusion technique using small unilamellar vesicles (SUVs). (i) Approach, (ii) Fusion, (iii) Flattening, iv) Expansion/sliding, and (v) SLB	5
Figure 4.1 Standard curve for DMPC quantification	16
Figure 4.2 Standard curve for enzyme quantification	17
Figure 4.3 Standard curve for glucose quantification	18
Figure 4.4 Standard curve for H ₂ O ₂ quantification	19
Figure 4.5 Standard curve for ABTS ABTS ⁺⁺ quantification	20
Figure 4.6 Schematic diagram of experimental set up	22
Figure 4.7 Schematic representation of biomimetic nylon membrane pores. 1. Functionalization of membrane pores by direct lipid bilayer deposition (L), 2. Functionalization of membrane pores by immobilization of polymer cushion-supported lipid bilayer (CL)	24
Figure 5.1. Representative DLS profile of SUVs of DMPC. DMPC concentration of SUV solution was 0.67 mg/mL in 0.1 M NaCl	29
Figure 5.2. AFM images of SUVs of DMPC. DMPC concentration was 0.67 mg/mL in 0.1 M NaCl	30
Figure 5.3. Nile Red fluorescence of SUVs of DMPC. DMPC concentration was 0.67 in 0.1 M NaCl, Nile Red concentration was 1 mg/mL	31
Figure 5.4 Activity study of immobilized GOx within pores of B (Bare nylon membrane), L (Lipid deposited membrane) and CL (Polymer cushioned lipid deposited membrane). Errors bars shown are in standard deviation.(Conditions: Flow rate 2 mL/min, substrate concentration 15 mM, pH 6.5)	34
Figure 5.5. Activity study of GOx immobilized on surface and within pores of cushioned lipid deposited membranes (CL). Errors bars shown are in standard deviation. (Conditions: Flow rate 2 mL/min, substrate concentration 15 mM and pH 6.5)	36
Figure 5.6 Effect of residence time (i.e. flow rate) on production of H ₂ O ₂ and rate of H ₂ O ₂ production for 15 mM glucose solution by GOx immobilized within the pores of CL nylon membrane. (Conditions: amount of immobilized GOx 700 µg, pH 6.5, temperature 25 °C, and residence time 0.108 – 0.018 min)	39

Figure 5.7. Effect of pH on activity of free GOx and GOx immobilized within pores of CL membrane. Activity was calculated based on the concentration of H ₂ O ₂ produced and was normalized on the basis of the maximum activity. (Conditions: Maximum activity of free GOx 39 μM H ₂ O ₂ /μg of GOx, maximum activity of immobilized GOx 1.27 μM H ₂ O ₂ / μg of GOx, amount of GOx immobilized 700 μg, residence time 1.62 s, external membrane area 4.9 cm ² , membrane thickness 160 μm, temperature 25 °C and concentration of glucose 15 mM)	40
Figure 5.8. Storage stability of free GOx and GOx immobilized within the pores of CL membrane over a period of 28 days. Activity was calculated based on the concentration of H ₂ O ₂ and was normalized by dividing with the activity on the first day	41
Figure 5.9. Co-immobilization of GOx (★) and HRP (✦) enzymes within CL membrane	42
Figure 5.10 Activity of immobilized HRP enzyme within pores of B, L and CL membranes. Data points are represented by the mean ± standard deviation for n=3. (Conditions: Flow rate 2 mL/min, ABTS concentration 3 mM, H ₂ O ₂ concentration 1.3 mM, pH 6.5)	44
Figure 5.11. Amount of immobilized GOx and HRP within B (blank), L (lipid bilayer deposited) and CL (polymer cushion supported lipid bilayer attached) membrane pores. CL-C represents co-immobilized GOx and HRP enzymes within the same CL membrane. Data points are represented by the mean ± standard deviation for n=3. (Conditions: Flow rate 2 mL/min, pH 6.5)	45
Figure 5.12. Activity of CL-S and CL-C bienzymatic systems. Enzymes were immobilized within the pores of CL membrane. Data points are represented by the mean ± standard deviation for n=3. (Conditions: Flow rate 2 mL/min, glucose concentration 15 mM, ABTS 3 mM, pH 6.5)	47
Figure 5.13. Effect of pH on activity of free enzymes and CL-C configuration. Activity was normalized on the basis of the maximum activity. Data points are represented by the mean ± standard deviation for n=6 (Conditions: External membrane area 4.9 cm ² , thickness of one membrane 160 μm, concentration of glucose 15 mM, concentration of ABTS 3 mM)	49
Figure 5.14. Stability of free enzymes and immobilized GOx-HRP within the pores of CL membrane over a period of 28 days. Activity was calculated and normalized by dividing with the activity on the first day	51
Figure 5.15 Schematic representation of multienzymatic system	52
Figure 5.16 Activity of multienzymatic system containing immobilized GA and coimmobilized GOx+HRP enzymes within CL membrane. (Conditions: Flow rate 2 mL/min, ABTS concentration 3 mM, H ₂ O ₂ concentration 1.3 mM, pH 6.5)	54

Figure 5.17. Activity of free and immobilized GA within CL membrane at different pH	55
Figure 5.18 Stability of free and immobilized GA within the pores of CL membrane over a period of 28 days. Activity was calculated and normalized by dividing with the activity on the first day	56
Figure 5.19. Schematic representation of formation of reversibly attached phospholipid bilayer (SLB) functionalized nylon membrane pores containing electrostatically immobilized GOx followed by sequential detachment of GOx and SLB	57
Figure 5.20. Continuous production of hydrogen peroxide by oxidation of glucose using electrostatically immobilized fresh GOx within reused membrane	58
Figure 5.21 ^1H NMR spectrum of DMPC solutions at 25 °C	59
Figure 5.22. TEM micrographs for steps of SLB formation on TEM copper grid using a. stock DMPC solution before attachment, and b. detached DMPC solution	60



Chapter 1: Introduction

Recent years have witnessed a major thrust in moving towards sustainable bio-based economy utilizing renewable resources and adopting green technologies. Enzymes and enzymatic processes play a major role in achieving that goal. Enzymes are highly selective in nature and involve environment friendly processes. Hence, they are often preferred over chemical catalysts; however, their applications in industrial scale are limited by several factors, including the high cost, sensitivity towards the operating conditions and lack of reusability.

Enzymatic catalysis by free enzyme offers higher initial activity, but suffers from some major drawbacks, such as, lack of reusability, difficulty in downstream processing and low operational stability [1]. This led to the development of technologies for enzyme immobilization to improve long-term operational stability and cumbersome recovery and reuse of enzymes without major compromise in activity. One of the major concerns in enzyme immobilization is the reduced activity of enzyme, which occurs because of the blockage of the active sites due to the close proximity to the support material [2]. An approach to circumvent this problem is the immobilization of enzyme on a functionalized support matrix, which keeps the enzyme away from the base support material and allows post-immobilization arrangement of enzyme. Another major challenge with immobilized enzyme is the slow kinetics of reaction due to the unfavorable hydrodynamics under diffusive mode of flow through a porous media [3]. Therefore, a support material that offers improved hydrodynamics without compromising the activity is of great interest to the scientific community.

Biological membranes are semi-permeable and exceptionally selective with high transport rates [4]. Phospholipids are one of the major constituents of the biological membranes, where they exist as functional bilayer, known as lipid bilayer. The structure of lipid bilayer is self-assembled, and a remarkable balance among electrostatic, hydration, steric and long-range van der Waals forces provides the stability to it [5]. In order to mimic biological systems, lipid bilayer has been deposited on solid surfaces, known as supported lipid bilayer (SLB) [6]. SLB formation by spontaneous fusion of small unilamellar vesicles (SUVs) or liposome fusion on appropriate solid

surfaces, also known as Vesicle-Fusion (VF) method, has been extensively practiced, mainly because of the ease of formation [7–11]. For the formation of SLB on solid support, SUVs approach towards the support and get attached to the surface. After attachment, it begins to flatten from the edges. The outer, flattened areas expand and spread resulting into a partially flattened liposome. The liposome collapses to form two bilayers stacked on top of each other. The uppermost bilayer moves from the lower one to unoccupied areas on the surface. This movement can occur by two mechanisms, rolling in and sliding, resulting in a single bilayer structure [12].

Biomimetic membranes have wide range of applications, such as, sensor development, ligand-receptor studies, cell signaling, immobilized enzymatic catalysis, etc [13–15]. The fluid nature of SLB allows post-immobilization arrangement of enzyme, thereby improving the activity of enzyme [16]. As support material for SLB formation, polymeric membranes appear to be a suitable candidate. These membranes, being porous in nature, provide high surface area, improve the stability of immobilized enzymes and offer reusability and continuous production under pressure-driven conditions [17–19]. Membrane technology provides opportunity for easy scale-up with high-quality products. They are, in general, energy-efficient and environment friendly and have wide range of applications [20–22]. Membranes can be modified in various ways to impart the desired functionalities, thereby offering versatility in properties and structures [23–30].

Functionalized membranes can be used in many pressure driven processes, such as, water treatment and purification, pharmaceuticals processing, filtration of non-biodegradable and highly toxic inorganic micropollutants, chemical, medical, textile and petrochemical processing, biotechnology, enzyme immobilization and environmental studies, etc. [31–35].

Functionalization of pores of membranes provides an additional advantage of extended functionalization matrix as compare to surface functionalization [36]. Immobilization of enzymes in functionalized membranes allows high enzyme loading, leads to simpler downstream processing and provides improved stability and reusability. They also provide opportunity for control over critical operational parameters, such as residence time [37,38].

In this study, we have integrated the benefits of phospholipid bilayer and microporous structure of polymeric membranes within a single configuration and developed phospholipid bilayer functionalized biomimetic membrane pores for efficient enzymatic catalysis. We

hypothesized that the structural and functional characteristics of the phospholipid bilayer will remain intact within the membrane pores under pressure-driven convective flow. To the best of our knowledge, this is the first study on development of SLB within functionalized membrane pore.



Chapter 2: Literature Review

Supported lipid bilayer (SLB) is composed of two layers of phospholipid molecules supported on a suitable underlying surface and provides native environment to different types of biomolecules [39]. SLB has attracted wide attention from scientific community by virtue of their stability and fluidity to mimic biological cell membranes [40], fluidity being its most striking property. The fluid nature of lipid bilayer is due to the ability of diffusion of both of the constituent layers over the entire support surface.

The structure of lipid bilayer is self-assembled, and a remarkable balance among electrostatic, hydration, steric and long-range van der Waals forces provides the stability to it [5]. Formation of SLB is a spontaneous process, which occurs essentially by two techniques – Langmuir–Blodgett (LB) and Vesicle-Fusion (VF). The latter one, which involves fusion of small unilamellar vesicles (SUVs), has the advantages of versatility and simplicity over LB technique [41].

SUVs are spherical, enclosed structure of lipid bilayer. SLB formation by spontaneous fusion of small unilamellar vesicles (SUVs) or liposome fusion on appropriate solid surfaces (e.g. silicon, silica, quartz etc.), is known as VF method and has been extensively practiced, mainly because of the ease of formation [7–11,42]. The essence of the mechanism is illustrated in Figure 2.1. SUVs from solution phase, when spread onto a solid surface, approach towards each other, fuse and flatten to form liposomal structure. Then, the liposomal structure ruptures on both ends resulting into two lipid bilayers, one above the other. Two lipid bilayers slide on opposite directions to expand and eventually lead to bilayer formation. This movement can occur by two mechanisms, rolling in and sliding, resulting in a single bilayer structure [12]. Single SUV could also lead to SLB formation following the above mentioned mechanism.

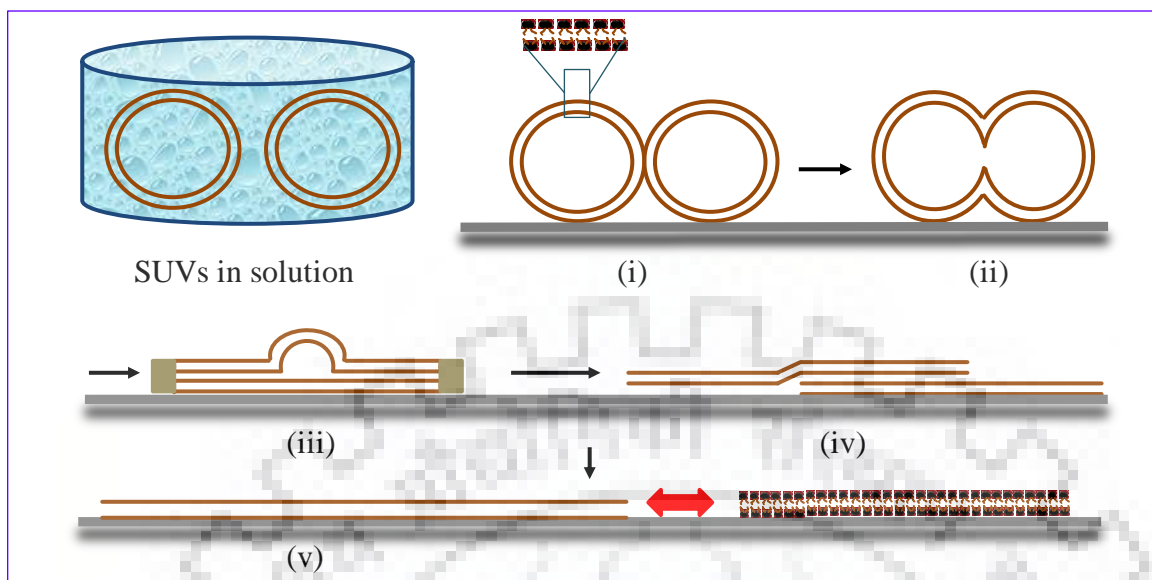


Figure 2.1. Mechanism of supported lipid bilayer (SLB) formation on a solid surface following Vesicle-Fusion technique using small unilamellar vesicles (SUVs). (i) Approach, (ii) Fusion, (iii) Flattening, (iv) Expansion/sliding, and (v) SLB

Selection of support material for SLB formation is very crucial as some of them (e.g. aluminium oxide) can restrict vesicle fusion and hence hinder continuous lipid bilayer formation, while others (e.g. Indium Tin Oxide) can prevent lateral diffusion and hence reduce mobility (fluidity) [5]. To circumvent these effects, one approach can be the incorporation of polymer cushion or polyelectrolyte layer between the support surface and lipid bilayer [43–45]. The space (water layer) between the solid surface and lipid bilayer of SLB is 1–2 nm, which can be extended to several nanometers by incorporating polymer cushion [46]. This polymer cushion acts as a hydrophilic lubricant, is deformable and mobile, and hence acts as a suitable support for fluid lipid bilayer membrane formation [11].

Yue-xiao et al. (2014) have done extensive research on the importance of lipid bilayer for the development of biomimetic systems. In their review, they have discussed different strategies of biomimetic membrane development to improve the transport efficiency and specificity in separation processes [4]. Supported lipid bilayer (SLB), has got a wide range of applications. Examples include development of drugs targeting cell surface, [47,48] monoclonal antibody

development [49–51] disease cell recognition by using nanoparticles [52], designing biocompatible interfaces for enzyme immobilization, biosensor development, lipid-protein interaction, [53,54] etc. Crites et al. (2016) prepared glass-supported lipid bilayers used to study immune synapse formation by Jurkat cells. They also used silica beads supported lipid bilayers for the study of signaling responses by western blotting, flow cytometry and gene-expression analysis [55].

Enzymes are of utmost importance in various industries due to their high specificity and environment friendliness. By 2020, the global market for industrial enzymes is expected to reach 6.2 Billion USD, in which share of India is expected to be around 361 million USD [56]. Lipid bilayer, entered into the realm of immobilized enzyme quite late, was able to draw significant attention from the scientific community and emerged as one of the front runners for immobilizing enzymes, particularly for sensing applications [57,58]. The fluid nature of SLB allows post-immobilization arrangement of enzyme, thereby improving the activity of enzyme [16].

Moreover, increased space due to polymer cushion prohibits direct contact between immobilized enzymes and substrate surface, which in turn helps to circumvent the loss of active sites of enzymes [16]. While using the lipid bilayer for enzymatic catalysis, the flexibility to change the composition of lipid bilayer by using different types of lipids makes the whole process compatible for different enzymes [59]. Lewis et al. (2006) developed a biosensor by immobilizing bovine cytochrome c oxidase (CCO) into supported lipid bilayer [60]. CCO is the terminal electron acceptor in the mitochondrial electron transport chain and is responsible for greater than 90 % of cellular oxygen consumption in its role of producing cellular ATP. *In vivo* CCO is responsible for the four electron reduction of molecular oxygen to water. It was observed that the sensor performs in a manner which is expected of the native enzyme. Phosphatase enzymes were immobilized in phospholipid bilayer-coated microcapillary tubes and microfluidic channels by Mao et al. (2002) with the enzyme turnover number of $51.1 \pm 3.2 \text{ s}^{-1}$ [61].

There are many reactions that involve more than one enzyme [62]. Glucose oxidase and glucoamylase were non-covalently immobilized on chemically reduced graphene oxide for the conversion of starch into gluconic acid in one pot by Zhao et al in 2014 [63]. In 2007, Logan et al. studied the co-immobilization of (i) two enzymes (glucose oxidase and horseradish peroxidase) and (ii) three enzymes (Invertase, Glucose oxidase and horseradish peroxidase) in porous polymer

monoliths in microfluidic devices. by [64]. Some studies have even reported the superior catalytic properties of co-immobilized enzyme systems over the successive use of two individual enzymes [65].

There are many reactions that involve more than one enzyme [62]. Immobilization of more than one enzyme can be achieved by covalent attachment as well as non-covalent methods. Covalent methods, on one hand, increase the stability of enzyme, but, on the other hand, compromise substantially on the activity of enzyme. Non-covalent methods, such as electrostatic interaction, reduce the negative impact of immobilization on enzyme activity, while maintaining satisfactory stability [3].

Glucose oxidase and glucoamylase were non-covalently immobilized on chemically reduced graphene oxide for the conversion of starch into gluconic acid in one pot by Zhao et al in 2014. The yield of gluconic acid was reported to be around 82 % and residual activity was observed to be 85 % after four cycles [63]. In 2006, nitrobenzene nitroreductase and glucose-6-phosphate dehydrogenase were co-encapsulated by Betancor et al. in silica particles to convert nitrobenzene to hydroxylaminobenzene along with the recycling of nicotinamide adenine dinucleotide phosphate [66]. In 2007, Logan et al. studied the co-immobilization of (i) two enzymes (glucose oxidase and horseradish peroxidase) and (ii) three enzymes (Invertase, Glucose oxidase and horseradish peroxidase) in porous polymer monoliths in microfluidic devices by photopatterning method using covalent attachment. The flow-through mode was used for analysis of catalytic activity and at higher flow rates, mass transfer limitations were reported to be absent [64]. Some studies have even reported the superior catalytic properties of co-immobilized enzyme systems over the successive use of two individual enzymes [65].

However, development of immobilized enzymatic system involving more than one enzyme has certain crucial limitations. The optimization of operating conditions after immobilization depends on the cooperating enzymes. Therefore, the study of overall reaction kinetics, mass transfer, interaction of substrates, coupling pH and coupling temperature become more complex compare to single enzyme system. All these parameters influence the overall immobilization strategy. Moreover, preservation of the catalytic activity and improved stability of all the constituent enzymes are two major challenges during the immobilization of more than one enzyme using same support matrix [67]. Due to these limitations and challenges, immobilization of more

than one enzyme requires better strategy to provide simple and facile procedure, which can enable low mass transfer resistance and absence of enzyme leakage, while maintaining the catalytic activity of constituent enzymes and overall operational and storage stability.

Enzymatic catalysis by free enzyme offers higher initial activity, but suffers from some major drawbacks, such as, lack of reusability, difficulty in downstream processing and low operational stability [1]. These properties of immobilized enzymes facilitate the designing of bioreactors and improve the economy of industrial operations [68]. This led to the development of technologies for enzyme immobilization to improve long-term operational stability and cumbersome recovery and reuse of enzymes without major compromise in activity. The exploration of novel immobilization methods by using different support materials and matrices with enhanced overall performance is a matter of significant interest in research world [69].

One of the major concerns in enzyme immobilization is the reduced activity of enzyme, which occurs because of the blockage of the active sites due to the close proximity to the support material [2]. An approach to circumvent this problem is the immobilization of enzyme on a functionalized support matrix, which keeps the enzyme away from the base support material and allows post-immobilization arrangement of enzyme. Another major challenge with immobilized enzyme is the slow kinetics of reaction due to the unfavorable hydrodynamics under diffusive mode of flow through a porous media [3]. Therefore, a support material that offers improved hydrodynamics is of great interest to the scientific community.

Selection of support material for SLB formation is very crucial as some of them (e.g. aluminium oxide) can restrict vesicle fusion and hence hinder continuous lipid bilayer formation, while others (e.g. Indium Tin Oxide) can prevent lateral diffusion and hence reduce mobility (fluidity) [5]. To circumvent these effects, one approach can be the incorporation of polymer cushion or polyelectrolyte layer between the support surface and lipid bilayer [43–45]. The space (water layer) between the solid surface and lipid bilayer of SLB is 1–2 nm, which can be extended to several nanometers by incorporating polymer cushion [46]. This polymer cushion acts as a hydrophilic lubricant, is deformable and mobile, and hence acts as a suitable support for fluid lipid bilayer membrane formation [11]. Moreover, increased space due to polymer cushion prohibits direct contact between immobilized enzymes and substrate surface, which in turn helps to circumvent the loss of active sites of enzymes [16]. While using the lipid bilayer for enzymatic

catalysis, the flexibility to change the composition of lipid bilayer by using different types of lipids makes the whole process compatible for different enzymes [59].

As support material for SLB formation, commercial polymeric membranes are of growing interest in recent times. These porous membranes provide high surface area and enable continuous process under pressure-driven conditions [17]. Polymeric membranes can be functionalized using different chemistries to impart versatility in properties and structures [70]. Incorporation of a polymer cushion between the underlying support surface and overlaid SLB provides a tunable, mobile and soft hydrophilic substrate between the surface and SLB, and circumvents the influence of support surface on SLB functionality [11]. This polymer cushion can also serve as extended spacer arm and helps in avoiding direct contact between immobilized enzymes on SLB and support surface [2]. Functionalized membranes also allow high enzyme loading and provide opportunity for control over critical operational parameters, such as residence time [37,38]. Enzymes can either be immobilized together on same membrane or on different membranes separately [70]. Membrane surface modifications for enzyme immobilization have been studied widely. Compare to membrane surface modifications, studies involving membrane pore modifications are limited in numbers [3].

Membranes have emerged as a favorable support material for enzyme immobilization primarily due to their high surface area (microporous structure) and low mass-transfer resistance (pressure-driven convective flow). Functionalized membranes permit high enzyme loading, offer protective environment to immobilized enzymes and provide opportunity for modification in the critical operational parameters, such as residence time [21,38,71]. Membrane surface modifications for enzyme immobilization have been studied widely. Immobilization of trypsin on IAV membrane (modified PVDF membrane) was studied by Bienvenut et al. (1999). The amount of immobilized trypsin was reported to be $0.90 \pm 0.20 \mu\text{g}/\text{cm}^2$. In this study, the activity of immobilized trypsin was found to be stable upto 1 year when membranes were stored in 46 mM Tris-HCl, 1 mM CaCl_2 and 0.1 % azide buffer at 4 °C. The reusability of membranes had also been reported with a slight decrease in activity after at least 3 uses [72]. Covalent immobilization of glucose oxidase on microporous membrane, prepared from the acrylic acid (AAc) graft-copolymerized poly(vinylidene fluoride) (PVDF) was studied by Ying et al. (2002) [73]. The amount and activity of covalently immobilized enzyme was found to increase linearly with the

surface-graft concentration of the AAc-g-PVDF membranes. The amount of immobilized GOx was estimated to be $270 \mu\text{g}/\text{cm}^2$ for a graft concentration of about 0.97. Immobilized enzyme molecules were reported to retain about 55 % of their original activity after 60 days, whereas free enzymes could retain less than 35 % activity for the same period of time. Rauf et al. (2006) studied the immobilization of glucose oxidase on cellulose acetate-polymethylmethacrylate (CA-PMMA) membrane. The immobilized glucose oxidase enzyme was reported to retain 94 % of activity after 1 month storage period with a higher thermal stability (retained 46 % of the original activity at 70°C) [74]. Hilal et al. (2006) reported the immobilization of lipase enzyme by (i) adsorption on membranes, (ii) inclusion of enzyme in membrane structure by filtration and (iii) covalent attachment of lipase to membrane. For this study, two types of membranes, ultrafiltration membranes made of regenerated cellulose and polyethersulphone were used. Enzyme loading was reported to be in the range of $3.4\text{--}68 \mu\text{g proteins}/\text{cm}^2$ of external membrane area. Catalytic activity of immobilized lipase in terms of oleic acid conversion was approximately 18 % (enzyme loading: $0.6 \pm 0.05 \mu\text{g}/\text{cm}^2$) for covalently immobilized lipase without spacer, whereas approximately 21 % (enzyme loading: $0.9 \pm 0.1 \mu\text{g}/\text{cm}^2$) for covalently immobilized lipase with spacer. This was an important observation, which showed that the introduction of a spacer arm had an effect on the enzymatic activity. Spacer arm helped in maintaining the enzyme structure by minimizing the interaction between membrane surface and lipase [75].

Compare to membrane surface modifications, studies involving membrane pore modifications are limited in numbers. In 2008, layer-by-layer approach (nylon-based membrane matrix) and in-situ polymerization (PVDF membrane) approach within membrane pores for enzymatic catalysis was reported by Datta et al. [3]. Glucose oxidase was immobilized electrostatically within functionalized domains of PVDF membrane, while functionalized nylon membrane domains were used both for electrostatic as well as covalent immobilization of glucose oxidase. Electrostatically immobilized glucose oxidase enzyme within functionalized PVDF membrane domains was reported to have an activity of $17 \text{ mM H}_2\text{O}_2/\text{mg GOx}/\text{min}$. The activity was further reduced to only 80 % after 28 days of storage. Substantial research in the field of membrane pore functionalization has been done in Bhattacharyya laboratory at the University of Kentucky, USA [76].

There are various strategies to immobilize enzymes within membranes, e.g. covalent bonding, electrostatic interaction, layer-by-layer sequential deposition, etc. Enzymes can either be immobilized together on same membrane or on different membranes separately [70,77]. In 2003, Godjevargova et al. used glucose oxidase and catalase enzymes for covalent immobilization on chemically modified acrylonitrile copolymer ultrafiltration membrane. The catalytic efficiency of co-immobilized system was observed to be higher than glucose oxidase enzyme [78]. Nguyen and Yang developed combined cross-linked enzyme aggregates (combi-CLEA) using glucose oxidase (GOx) and horseradish peroxidase (HRP). They have concluded that due to co-immobilization, the distance between GOx and HRP decreased. This reduced the decomposition of the reaction intermediate hydrogen peroxide [79].

As support material, commercial polymeric membranes are of growing interest in recent times. Membrane technology can provide certain advantages to the bioprocess industries in the form of immobilized enzymes [21]. Porous membranes provide high surface area, improve the stability of immobilized enzymes and offer reusability and continuous production under pressure-driven conditions [17]. These membranes can be functionalized using different chemistries to impart versatility in properties and structures [70]. Functionalized membranes allow high enzyme loading and provide opportunity for control over critical operational parameters, such as residence time [37,38]. There are various strategies to immobilize enzymes within membranes, e.g. covalent bonding, electrostatic interaction, layer-by-layer sequential deposition, etc.

Enzymes can either be immobilized together on same membrane or on different membranes separately [70]. In 2003, Godjevargova et al. used glucose oxidase and catalase enzymes for covalent immobilization on chemically modified acrylonitrile copolymer ultrafiltration membrane. The catalytic efficiency of co-immobilized system was observed to be higher than glucose oxidase enzyme [78]. Nguyen and Yang developed combined cross-linked enzyme aggregates (combi-CLEA) using glucose oxidase (GOx) and horseradish peroxidase (HRP). They have concluded that due to co-immobilization, the distance between GOx and HRP decreased. This reduced the decomposition of the reaction intermediate hydrogen peroxide [79]. Direct immobilization of enzymes on membranes can cause changes in conformation and/or blockage of active sites. The direct contact can be minimized by using some matrix, which functions as spacer arm between membrane and enzyme [2]. The spacer arm can be introduced by

modifying membrane before enzyme immobilization. Membrane surface modifications for enzyme immobilization have been studied widely. Compare to membrane surface modifications, studies involving membrane pore modifications are limited in numbers [3].

The overall process of enzyme immobilization can be even more efficient if the support matrix could also allow post-immobilization rearrangement of enzyme. Supported lipid bilayer (SLB), being fluid in nature, is one such matrix [16]. SLB contains some key properties of biological cell membrane, and hence, is an ideal candidate for mimicking the native environment for enzyme immobilization. Strategies to develop biomimetic membrane system based on lipid bilayer, to improve the separation processes and transport efficiencies, was reviewed by Yue-xiao et al. in 2014 [4]. Tabaei et al. (2016) demonstrated multienzyme catalytic phosphorylation of phosphatidylinositol (PI) in a supported lipid bilayer membrane. In this study, the generation of PI-4,5-bisphosphate was investigated by sequential treatment of a PI-containing bilayer with PI 4-kinase III β followed by PIP 5-kinase [78]. The formation of continuous SLB occurs spontaneously by Vesicle-Fusion method and is a highly stable structure. Incorporation of polymer cushion provides a tunable, mobile and soft hydrophilic substrate between the support surface and SLB, and circumvents the influence of support surface on SLB functionality [11]. This polymer cushion can also serve as extended spacer arm and helps in avoiding direct contact between enzymes and support surface [2]. Moreover, the flexibility of maintaining the desired composition of lipids in the formation of SLB, provides an additional advantage of using SLB as matrix for immobilization of enzymes [59].

Chapter 3: Objectives

The overall objective was to develop novel functionalized membrane containing supported lipid bilayer. The developed biomimetic membrane was employed as a matrix for immobilized enzymatic catalysis. Following are the major objectives of the study:

1. Development of novel biomimetic membrane by functionalizing membrane pores with supported lipid bilayer
2. Application of the developed biomimetic membrane in immobilized enzymatic catalysis
3. Development of immobilized bienzymatic system supported on biomimetic membrane
4. Augmentation of the developed system in immobilized multienzymatic catalytic process
5. Evaluating the reusability of the functionalized membrane, supported lipid bilayer and immobilized enzymes

Chapter 4: Materials and Methods

This chapter contains detailed description of the equipments, materials, experimental methods and analytical procedures used for functionalization of membranes, formation of supported lipid bilayer, enzymatic catalysis, development of different enzymatic systems and reusability of developed functionalized membrane-SLB matrix.

4.1 Equipments

A steel membrane holder (25 mm disc diameter, dead-end type) was used to conduct experiments under convective mode of flow. Inlet and outlet of the membrane holder were connected to the feed tank and sample collection tank, respectively. To maintain the desired flow rate, a peristaltic pump with variable flow was used.

4.2 Materials

4.2.1 Membrane

Ultipor® Nylon 66 membrane discs (membrane diameter of 25 mm, pore diameter of 0.2 μm , average thickness of 160 μm), used for all the experiments, were purchased from Pall Corporation, USA (Product No. NR025100).

4.2.2 Chemicals

1,2-dimyristoyl-sn-glycero-3-phosphocholine (DMPC) was purchased from Avanti Polar Lipids, USA (Product No. 850345P). Epichlorohydrin (ECH, Product No. 027706) was purchased from Central Drug House (P) Ltd., India. Polyethyleneimine (PEI, Product No. 408727, MW ~25,000) and 15 % solution of titanium oxysulfate in dilute H_2SO_4 (Product No. 495379) were purchased from Aldrich Chemical Co., USA. β -D(+)-glucose (Product No. 20117) and sodium chloride (Product No. 20241) were purchased from s d fine-chem Limited, India. Enzymes, glucose oxidase from *Aspergillus niger* (GOx, Product No. RM7064, MW 160000) and horseradish peroxidase from horseradish (HRP, Product No. MB225, MW 44000) were purchased from HiMedia Laboratories, India. Glucoamylase enzyme from *Rhizopus sp.* (Product No. 28453,

MW 70000) was purchased from Sisco Research Laboratories, India. Soluble starch (Product No. S9765, MW 342.30) was purchased from Aldrich Chemical Co., USA. 2,2'-Azino-bis-(3-ethylbenzothiazoline-6-sulfonic acid) diammonium salt ABTS(NH₄)₂ (Product No. RM9270) and Bradford reagent (Product No. ML106-500ML) were also purchased from HiMedia Laboratories, India. All the experiments were conducted with ultrapure water.

All other chemicals used in the project were purchased from HiMedia Laboratories, India, unless stated otherwise.

4.3 Analytical procedures

For all spectrophotometric measurements of various liquid samples, ultraviolet-visible (UV-Vis) spectrophotometer (Varian, Cary 60) was used.

4.3.1. Quantification of Phospholipid: The amount of DMPC in a solution was determined by Stewart Assay [32]. This colorimetric method is based on the formation of a complex between phospholipids and ammonium ferrothiocyanate. To prepare ammonium ferrothiocyanate, 27 g of ferric chloride (FeCl₃.6H₂O) was mixed with 30 g of ammonium thiocyanate (NH₄SCN) in 1 L of water. Aliquots of DMPC solutions were left for complete evaporation of solvent. Then, DMPC residue was dissolved in 2 mL of chloroform and 1 mL of thiocyanate reagent was added to this. The mixture was vortexed for 1 min and centrifuged at 10000 rpm. Lower red layer (chloroform) was removed with a Pasteur pipette. Absorbance of this solution was taken at 488 nm and concentration of DMPC was determined with the help of a calibration curve prepared from known concentrations of standard DMPC solutions (Figure 4.1). The linear range for Stewart Assay used for this study was 10-70 µg/mL.

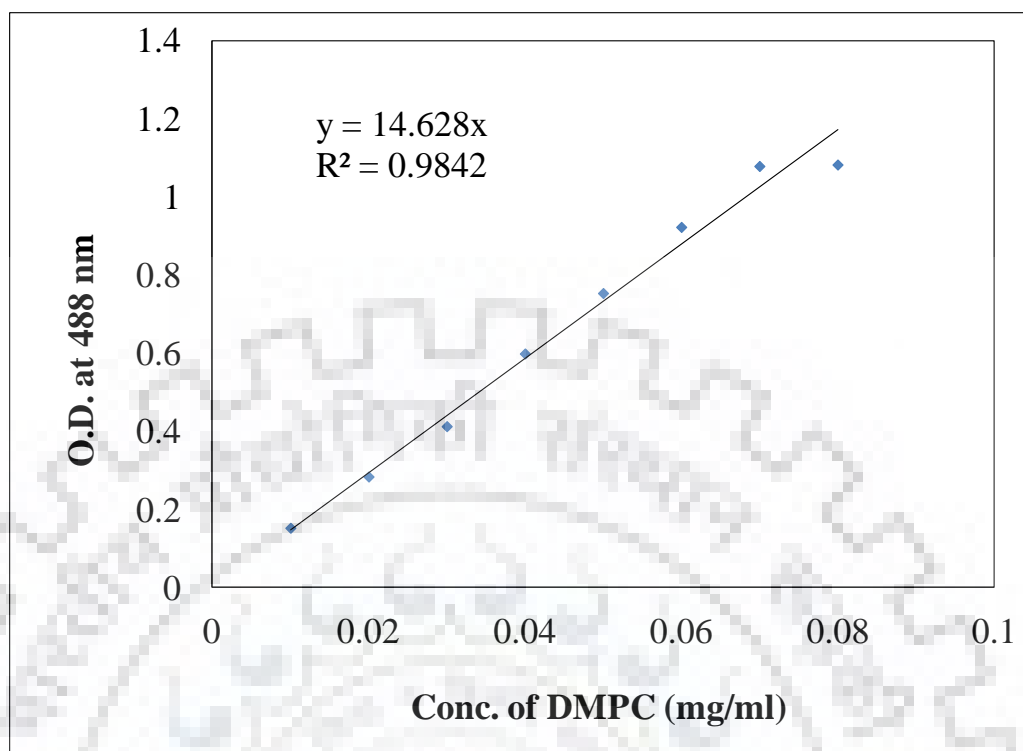


Figure 4.1 Standard curve for DMPC quantification

4.3.2. Quantification of enzymes: For the quantification of GOx and HRP enzymes, Bradford Protein Assay was used [80]. The Bradford assay, a colorimetric protein assay, is based on the formation of a protein-dye complex between protein in solution and a dye, Coomassie Brilliant Blue G-250. The absorption maximum of the dye shifts from 465 to 595 nm after the formation of protein-dye complex. Under acidic conditions, the red form of the dye is converted into blue form after binding to the protein being assayed. To quantify the immobilized enzyme, concentration of leftover enzyme in the solution after immobilization, concentration of enzyme in the washing solution (used to remove any unbound enzyme) and concentration of enzyme in the initial solution were analyzed. For the quantification of enzymes by Bradford Assay, 0.3 mL of enzyme sample was mixed with 3 mL of Bradford reagent. The enzyme-reagent mixture was vortexed and incubated at room temperature for 10 min. Absorbance was taken at 595 nm. The concentration of enzyme was determined with the help of a standard calibration curve, which was prepared from standard BSA solutions (Figure 4.2). The linear range of the Bradford Protein Assay was 1-20 $\mu\text{g/mL}$ in this study.

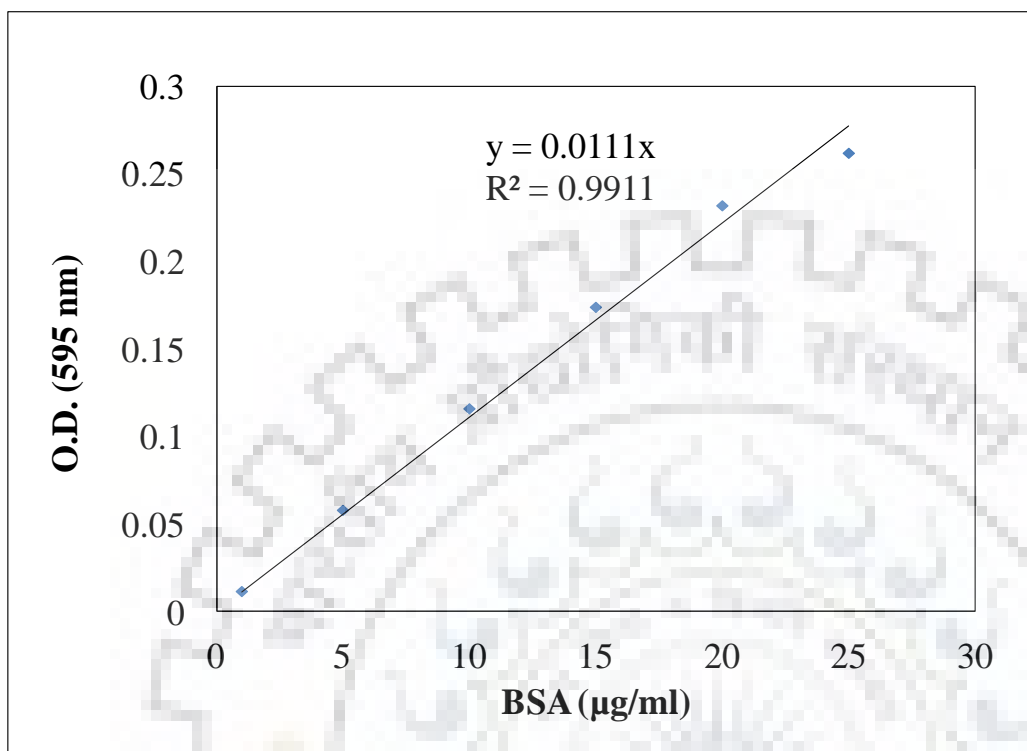


Figure 4.2 Standard curve for enzyme quantification

4.3.3. Quantification of glucose: Amount of glucose liberated by starch hydrolysis through glucoamylase (GA) catalysis was estimated by dinitrosalicylic (DNS) assay [81]. When alkaline solution of 3,5-dinitrosalicylic acid reacts with glucose, it is converted into reddish brown coloured complex, 3-amino-5-nitrosalicylic acid, which has an absorbance maximum at 540 nm. To quantify glucose in hydrolysed sample, 1 mL of sample was mixed with 3 mL of DNS reagent in a test tube. Test tube was covered and kept in boiling water bath for 5 min. Test tube was taken out, and while it is warm, 1 mL of 40 % potassium sodium tartarate solution was added to it. Mixture was cooled down to room temperature and absorbance was taken at 540 nm. Amount of glucose in the sample analyzed was estimated with the help of standard curve (Figure 4.3). The linear range of the DNS Assay was 50-300 µg/mL in this study.

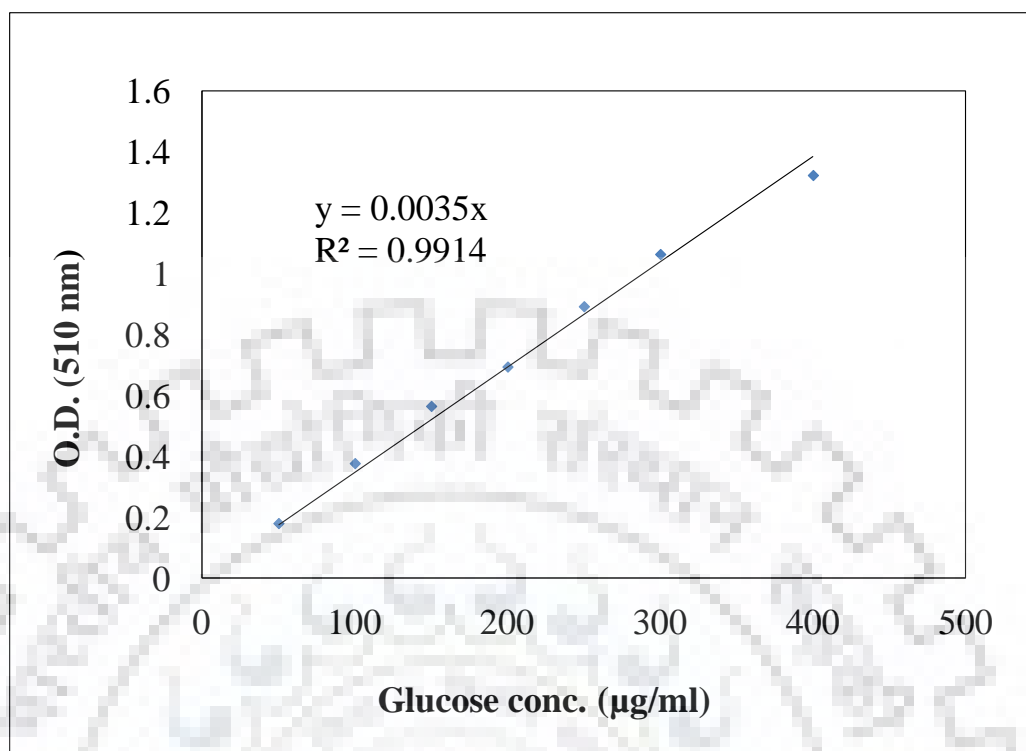


Figure 4.3 Standard curve for glucose quantification

4.3.4. Quantification of Hydrogen peroxide (H₂O₂): A colorimetric method described by Eisenberg [82] was used to analyze the concentration of H₂O₂ in solution. The assay is based on the spectrophotometric measurement of the color intensity of titanium oxysulfate reagent treated with H₂O₂ solution to form pertitanic acid (TiO₂·H₂O₂). To analyze H₂O₂ sample, 100 µl titanium oxysulfate was added to 900 µl sample. Mixture was vortexed and absorbance was taken at 407 nm. The concentration was determined with the help of a calibration curve, which was prepared from standard H₂O₂ (Figure 4.4). The linear range of H₂O₂ analysis by this colorimetric method was 0.03-3 mM in this study.

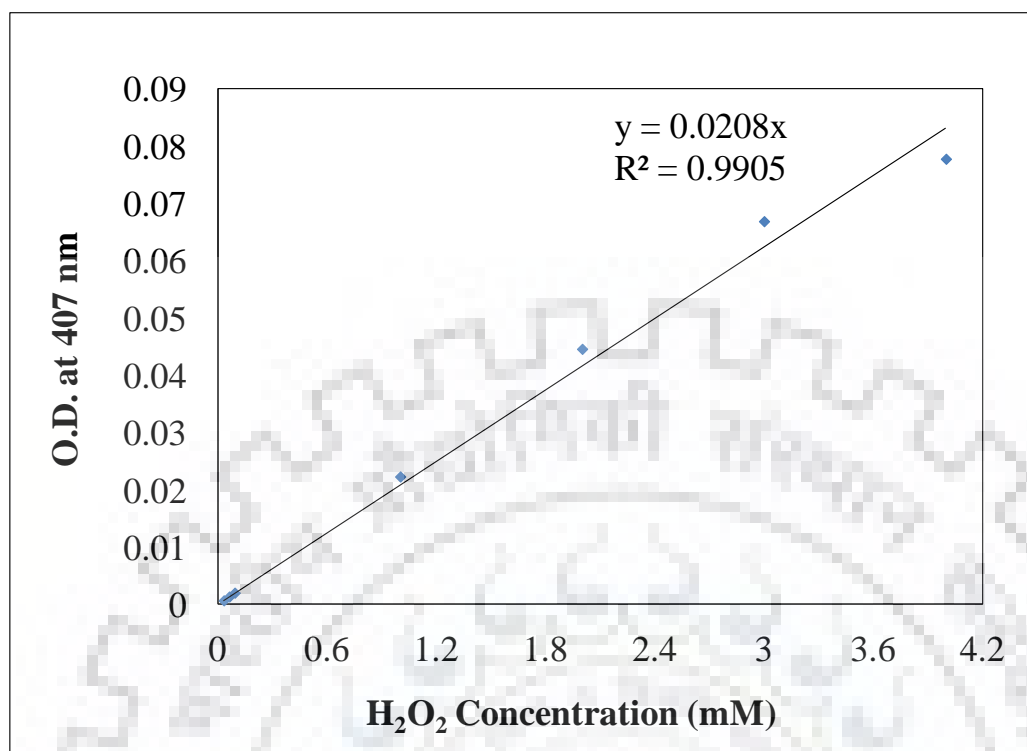


Figure 4.4 Standard curve for H₂O₂ quantification

4.3.5. Quantification of ABTS^{•+}: Activity of HRP was determined colorimetrically using ABTS and hydrogen peroxide as substrates. Two molecules of ABTS react with one molecule of H₂O₂ producing two molecules of ABTS^{•+} in the presence of HRP enzyme. ABTS has an absorption maximum at 340 nm, while for the ABTS-cationic radical (ABTS^{•+}) the maximum absorbance is obtained at 414 nm [9]. The concentration of ABTS^{•+} was calculated with the help of a standard calibration curve. The calibration curve was prepared using known concentrations of ABTS (Figure 4.5). The linear range of ABTS^{•+} analysis by this colorimetric method was 0.4-2 mM in this study.

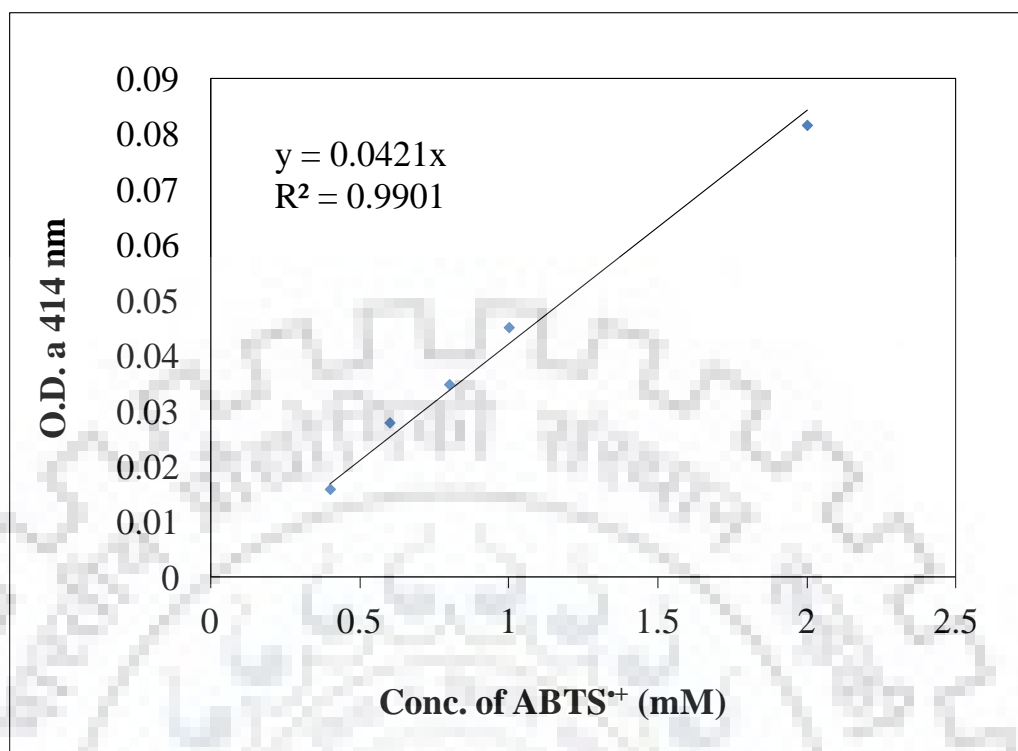


Figure 4.5 Standard curve for ABTS ABTS⁺⁺ quantification

4.3.6. Activity analysis of immobilized GOx: The activity of immobilized GOx was determined by measuring the concentration of H₂O₂ produced by oxidation of glucose (gluconic acid is the byproduct). All the activity measurement experiments were performed with 15 mM glucose solution saturated with O₂. O₂ is very important in the second step of the two-step reaction mechanism of the catalytic oxidation of glucose. Thus, to maintain the saturation condition of O₂ in the media throughout the reaction, the experiments were performed with oxygen saturated glucose solution. NaOH and HCl were used to adjust the pH of the solution, whenever needed. β-D(+)-Glucose is referred as glucose in the text.

4.3.7. Activity analysis of GOx-HRP bienzymatic system: The activity of immobilized GOx-HRP bienzymatic system was determined by permeating a feed containing 3 mM ABTS and O₂ saturated 15 mM glucose solution through the membrane. Immobilized GOx catalyzed the oxidation of glucose to H₂O₂. This internally produced H₂O₂ oxidized ABTS to ABTS⁺⁺ in the presence of HRP enzyme. Permeate samples were analyzed colorimetrically to determine the

concentration of ABTS^{•+} as discussed previously. For HRP immobilized membrane, the activity was determined by permeating a solution containing 3 mM ABTS and 1.3 mM H₂O₂ and measuring the concentration of ABTS^{•+} produced.

4.3.8. Activity analysis of GA-GOx-HRP multi-enzymatic system: For the analysis of multi-enzymatic system containing GA, GOx and HRP, a feed solution containing 150 mM starch and 3 mM ABTS solution saturated with O₂ was supplied through membranes containing immobilized enzymes. GA, being a starch-hydrolyzing enzyme, released glucose by cleaving-off the non-reducing ends of starch. Produced glucose was quantified by DNS assay to analyze the activity of immobilized GA. Glucose was subsequently oxidized by immobilized GOx to produce gluconic acid and H₂O₂. The activity of immobilized GOx was analyzed by estimating the concentration of H₂O₂ as described earlier. After that HRP enzyme catalyzed the reaction between ABTS and H₂O₂ to produce ABTS^{•+}. The activity of immobilized HRP was determined by measuring the concentration of ABTS^{•+} as discussed earlier.

4.4 Experimental Methods: The phase transition temperature between gel phase to liquid crystalline phase of DMPC is 23 °C [35]. Therefore, to retain DMPC in liquid crystalline phase, the temperature was kept constant at 30 °C (T>T_m) . All the experiments were performed in triplicate and the observed variations in experimental results are represented as the standard deviation. To establish statistically significant difference with 95 % confidence level between two given data, *p-value* was calculated [83] and included, wherever applicable. The details of the experimental set up and protocols are discussed below.

All convective mode experiments were performed in a membrane holder (25 mm disc diameter). A peristaltic pump was used to maintain constant flow rate. Inlet of the holder was connected to the feed tank containing the desired solution. Outlet of the membrane holder was used for sample collection (Figure 4.6).

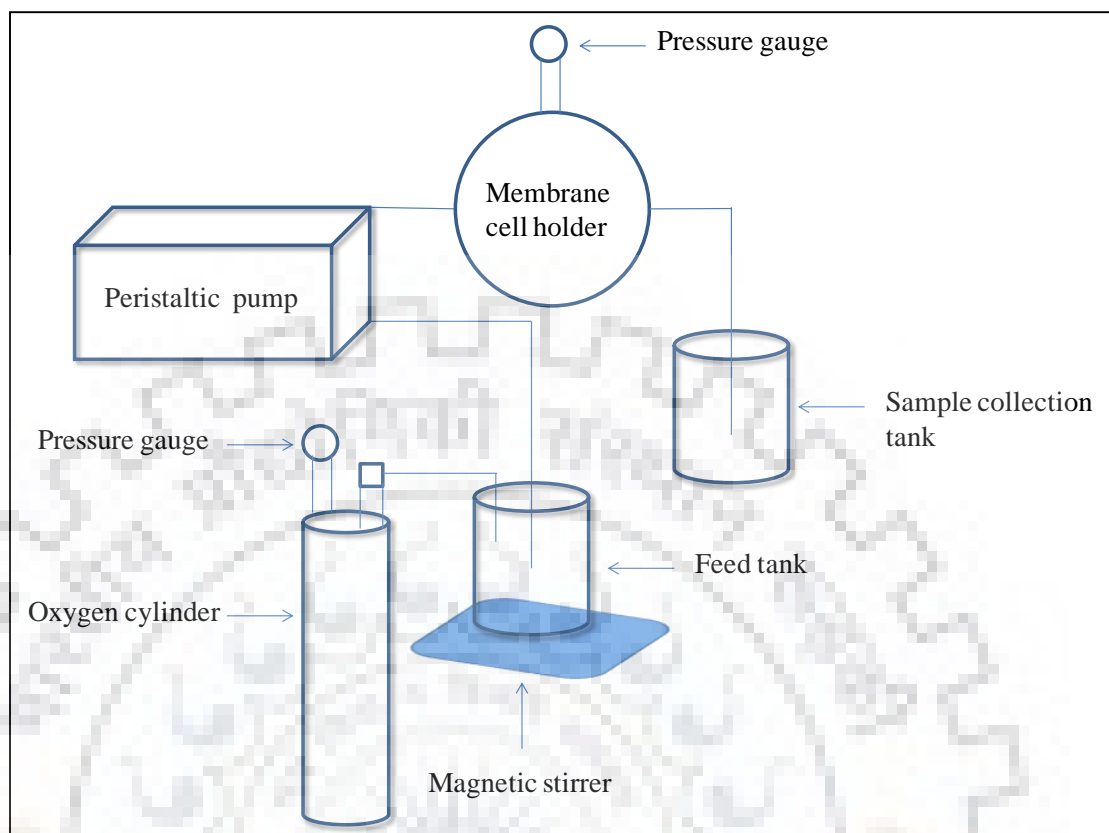


Figure 4.6. Schematic diagram of experimental set up

For the activity analysis of immobilized enzymes (GA, GOx, HRP, GOx-HRP bienzymatic system and GA-GOx-HRP multienzymatic system), continuous flow was maintained (unless stated otherwise). Activity analysis of free enzyme was conducted in batch mode. The porosity (ϵ) of the membrane was calculated with the help of the following equation:

$$\text{porosity } (\epsilon) = \text{Porous volume} / \text{Total volume}$$

To calculate porous volume, initial weight of a membrane was measured. Then, the same membrane was soaked overnight in ultrapure water. After taking out the membrane from ultrapure water, the membrane was wiped to remove residual surface water. Then, the final weight of the wet membrane was measured. The difference of the initial and final weight of the membrane divided with density of water gave porous volume of membrane as demonstrated below.

Porous volume (m^3) = total volume (v) \times porosity (ϵ) = (Weight after soaking - weight before soaking)/Density of water

Weight before soaking (initial weight of membrane) = 0.021 g, Weight after soaking (final weight of membrane) = 0.075 g

Therefore, porous volume = $(0.075 - 0.021) \text{ g} / 1 \text{ g.cm}^{-3} = 0.054 \text{ cm}^3 = 5.4 \times 10^{-8} \text{ m}^3$

Total volume = $\pi \times (\text{radius})^2 \times \text{thickness} = \pi \times (1.25 \times 10^{-2})^2 \times 160 \times 10^{-6} = 780 \times 10^{-10} \text{ m}^3$

i.e. Total volume of membrane = $7.8 \times 10^{-8} \text{ m}^3$

Therefore, porosity (ϵ) = Porous volume/Total volume = $5.4 \times 10^{-8} \text{ m}^3 / 7.8 \times 10^{-8} \text{ m}^3 = 0.7$

4.4.1. Preparation of small unilamellar vesicles (SUVs) from DMPC: DMPC was first dissolved in chloroform (1 mg/mL) and the mixture was kept overnight in vacuum oven at 40°C to evaporate extra solvent and form a thin lipid film of DMPC. The resultant lipid film was then hydrated with 0.1 M NaCl solution to get a final concentration of 0.7 mg/mL. The solution containing hydrated lipid film was then vortexed and sonicated (probe sonicator, 50 % duty cycle) for 20 min to form SUVs in solution. After sonication, the SUV containing solution was centrifuged at 10,000 rpm for 15 min to remove the aggregated phospholipids and other impurities. SUVs of desired size were collected in the supernatant of the centrifuge. Characterization of SUVs was done with the help of dynamic light scattering (DLS) system using Zetasizer Nano ZS90 and Nile Red fluorescence dye staining. Prepared SUVs were further used for lipid bilayer deposition within nylon membrane pores to develop biomimetic membranes.

4.4.2. Functionalization of membrane pore with lipid bilayer: Functionalization of membrane pores with lipid bilayer was accomplished by two different approaches using SUVs, (i) Direct deposition of lipid bilayer within bare membrane pores (Figure 4.7.a), and (ii) Formation of polymer cushion supported lipid bilayer within membrane pores (Figure 4.7.b).



Figure 4.7. Schematic representation of biomimetic nylon membrane pores. 1. Functionalization of membrane pores by direct lipid bilayer deposition (L), 2. Functionalization of membrane pores by immobilization of polymer cushion-supported lipid bilayer (CL).

Functionalization of pores of nylon membrane with direct deposition of lipid bilayer was achieved by Vesicle-Fusion method. The principle of Vesicle-Fusion method is briefly described in the Introduction section. Prior to functionalization with lipid bilayer, bare nylon membrane was conditioned with 50 mL ultrapure water. Then, 10 mL solution of SUVs was recirculated through the membrane for 45 min. After that the undeposited SUVs were removed from membrane pores by circulating 25 mL ultrapure water. A flow rate of 2 mL/min (convective mode) was maintained during the whole process using a peristaltic pump. Solutions of SUVs, before and after recirculation, and washing water containing the undeposited SUVs were subjected to colorimetric assay to quantify the amount of deposited DMPC within the lipid bilayer in membrane pores. Another set of experiments was conducted to study the deposition of phospholipid bilayer on membrane surface. For surface deposition of phospholipid bilayer, nylon membrane was soaked in 10 mL solution of SUVs for 45 min. After that the membrane was washed with 10 mL ultrapure water to remove undeposited SUVs. Deposited phospholipid was quantified as mentioned earlier.

In another approach, a polymer cushion was deposited prior to lipid bilayer formation within membrane pores. To deposit a polymer cushion, bare nylon membrane was first treated with HCl by recirculating 50 mL of 0.1N HCl for 45 min to expose the primary amine groups on membrane pore surface. After washing the membrane with ultrapure water, ECH (1 M, 50 mL) was passed for 45 min through membrane pores to introduce epoxide groups. Membrane was then washed with ultrapure water. Epoxide groups were then reacted with the amine groups by

permeating PEI (2 mM, 50 mL) for 45 min. After washing the membrane with ultrapure water, 10 mL of SUV solution was recirculated through the membrane for 45 min to ensure the saturation of the membrane by phospholipid. A flow rate of 2 mL/min (convective mode) was maintained during the whole process using a peristaltic pump. Phospholipid bilayer was formed on the PEI cushion following the Vesicle-Fusion method as described in Introduction section. Lipid incorporation within membrane pores was quantified as described earlier.

Electrostatic interaction between the positively charged secondary amine groups of PEI and the negatively charged phosphate groups of DMPC molecules resulted into polymer cushion supported lipid bilayer formation within membrane pores. Membrane containing only lipid bilayer and polymer cushion supported lipid bilayer will be referred as L and CL, respectively in further text. For CL membrane, a single amine group of nylon membrane was eventually transformed into multiple amine groups via PEI functionalization (polymer cushion) resulting into multiple sites for lipid bilayer immobilization. Consequently, covalently attached polymer cushion within CL membrane pores increased the hydrated space between the lipid bilayer and membrane pore surface by several nanometers from ~1–2 nm thin water layer present within L membrane [46]. This increased space helped in reducing the friction between membrane pore surface and lipid bilayer, which was otherwise present in L, and therefore, helped in maintaining the structural and dynamic integrity of the deposited lipid bilayer in CL as compared to L [84]. Moreover, the functionalized moieties of PEI chains provided an extended platform to lipid bilayer with significantly higher pore coverage in CL as compared to L membrane pores.

In another set of experiments, deposition of polymer cushioned phospholipid bilayer on membrane surface was conducted. For this, nylon membrane was first treated with 0.1N HCl to expose the primary amine groups on membrane surface by soaking the membrane in 50 ml of 0.1N HCl solution for 45 min. Then, the membrane was washed with ultrapure water and soaked in ECH (1 M, 50 mL) for 45 min to introduce epoxide groups. Again the membrane was washed with ultrapure water. Epoxide groups were then reacted with the amine groups of PEI by soaking the membrane in PEI (2 mM, 50 mL) solution for 45 min. After washing with ultrapure water, the membrane was then soaked in 10 mL of SUV solution for the formation of polymer cushioned lipid bilayer on membrane surface. Lipid deposition on membrane surface was quantified as described before. The covalently attached PEI functioned as the polymer cushion and the exposed

secondary amine groups of PEI served as the extended platform for subsequent phospholipid bilayer development.

4.4.3. Immobilization of enzyme (GA or GOx or HRP) within functionalized membrane pores: After functionalization of membrane pores with lipid bilayer, enzyme (GA or GOx or HRP) was immobilized within bare nylon membrane (B) or biomimetic membrane (L or CL). To immobilize enzyme, 10 mL of the desired enzyme solution (200 µg/mL) in ultrapure water at pH 6.5 was recirculated through the membrane pores. Flow rate was maintained at 2 mL/min and the time of recirculation was 45 min to ensure the saturation of the membrane by the enzyme. Any unbound enzyme was removed by washing with 25 mL of ultrapure water. Membranes containing immobilized enzyme(s) were stored at 4 °C. Depending upon pI, GA, GOx or HRP enzymes had positive or negative charge at pH 6.5 and therefore they attached electrostatically to counter charged groups (positively charged amine groups and negatively charged phosphate groups) of zwitterionic DMPC molecules of SLB.

4.4.4. Co-immobilization of GOx-HRP within biomimetic membrane: To co-immobilize GOx and HRP enzymes within the same CL membrane, first, GOx was immobilized within the pores by recirculating 10 mL of a 200 µg/mL GOx solution at pH 6.5. Then, the membrane was washed to remove any unbound GOx. This was followed by recirculation of 10 mL of 200 µg/mL HRP solution at pH 6.5 to immobilize HRP. Membrane containing co-immobilized GOx and HRP will be referred as CL-C in further text. The flow rate was maintained at 2 mL/min and time of recirculation was 45 min for each of the enzymes (to ensure the saturation of the membrane by enzymes). Membranes containing immobilized enzymes were stored at 4 °C.

4.4.5. Effect of residence time (i.e., flow rate) on activity: The effect of residence time on the activity of immobilized enzyme was studied by varying the volumetric flow rate of the feed for a fixed substrate concentration. For GOx, 15 mM glucose solution at pH 6.5 was used to study the effect of residence time on activity, while for GOx-HRP bienzymatic system, a feed solution containing 15 mM glucose solution and 3 mM ABTS solution at pH 6.5 was used. For GA-GOx-HRP multienzymatic system, a feed solution containing 150 mM starch solution and 3 mM ABTS solution at pH 6.5 was used for activity analysis. The flow rate was varied over a range of 0.5-3 mL/min.

4.4.6. Effect of pH on activity: The effect of pH on the activity of the immobilized GOx was studied by varying the pH over a range of 4-9 for 15 mM concentration of glucose solution at a constant flow rate of 2 mL/min. The effect of pH on the activity of GOx-HRP bienzymatic system was also studied by varying the pH of the substrate solution over a range of 4-9. 15 mM glucose solution along with 3 mM ABTS solution was used as feed solution at a constant flow rate of 2 mL/min. The effect of pH on the activity of GA-GOx-HRP multi-enzymatic system was also studied by varying the pH of the substrate solution over a range of 4-9. 150 mM starch solution along with 3 mM ABTS solution was used as feed solution at a constant flow rate of 2 mL/min. Permeate samples containing ABTS⁺⁺ were analyzed to determine the activity of the multi-enzymatic system. Homogeneous phase experiments for free enzymes (GA, GOx or HRP) were performed in batch mode with pH varying in the same range (4-9). To make the data comparable, normalized activity was calculated with respect to the highest activity obtained in each case.

4.4.7. Stability of the immobilized enzymatic system within functionalized membrane pores: The stability of different enzymatic systems (GOx, GOx-HRP bienzymatic system and GA-GOx-HRP multi-enzymatic system) within functionalized membranes was studied by measuring the activity after every 7 days for 28 days with intermediate storage at 4 °C. The same functionalized membrane(s) was used for the activity analysis of immobilized enzyme(s) at regular interval (i.e. on 0th day, 7th day, 14th day, 21st day and 28th day) in flow-through mode with the membrane held in membrane-holder (25 mm disc diameter) connected to a peristaltic pump. For all the experiments, flow rate of 2 mL/min was maintained. A glucose solution of 15 mM concentration (pH 6.5) was used for all stability studies of immobilized GOx. A feed solution containing 15 mM glucose solution along with 3 mM ABTS solution was used for all stability studies of GOx-HRP bienzymatic system and a feed solution containing 150 mM starch solution along with 3 mM ABTS solution was used for all stability studies of GA-GOx-HRP multi-enzymatic system. Collected samples (after 5 min, 10 min, 20 min and 30 min) were assayed colorimetrically and corresponding activity was calculated. To monitor any leakage of enzyme during stability studies, samples were collected and assayed colorimetrically.

For comparison, the stability of free enzymes (GA, GOx or HRP), was also studied over 28 days using stock solutions of GA, GOx or HRP. Individual samples were analyzed for activity of free enzymes. At regular interval (i.e. on 0th day, 7th day, 14th day, 21st day and 28th day) same

volume of enzyme (1 mL of 200 $\mu\text{g/mL}$) was taken out and mixed with 10 mL of corresponding substrate solution. For GOx, 15 mM glucose solution saturated with O_2 was used as substrate. For HRP, a substrate mixture containing ABTS (3 mM) and H_2O_2 (1.3 mM) was used, and for GA, 150 mM starch solution was used. Sample was collected and assayed colorimetrically. During all the experiments, same concentration and volume of free enzyme was used, therefore, the effect of loss of enzyme was nullified. The activity of immobilized enzyme was analyzed in flow-through mode and for free enzymes, batch mode was used. To make the data comparable, normalized activity was calculated with respect to the activity at $t=0$.

4.4.8. Reusability of the functionalized membrane and SLB: Reusability of the functionalized membrane and SLB was explored following a sequence of “attachment-detachment-reattachment”. The details of sequential attachment-detachment steps due to electrostatic interactions between the components are explained in results and discussion section.

To elute GOx, an eluent solution of dilute HCl with pH 3.5 was permeated through the membrane. SLB within the membrane remained intact as it was electrostatically attached to the PEI cushion under the above mentioned condition. Therefore, SLB functionalized membrane could be used repeatedly for enzyme immobilization. This approach of detachment of the electrostatically immobilized enzyme is useful to remove the deactivated enzyme and replenish the same membrane matrix with fresh enzyme. Alternatively, it can be implemented to immobilize different enzymes for different applications without changing the membrane matrix. After enzyme detachment, the SLB was detached by permeating an eluent solution (1 M NaCl, pH 11). Stock DMPC solution and detached DMPC solution were analyzed by ^1H NMR. For ^1H NMR analysis of DMPC, Deuterated chloroform (CDCl_3) was used as solvent. 0.1 mL of DMPC sample was mixed with 0.9 mL of solvent in NMR tube. Each sample was analysed after 512 scans.

Chapter 5: Results and Discussion

This chapter includes the results obtained for functionalizing nylon membrane pores with supported lipid bilayer (SLB) by incorporating phospholipid bilayer, electrostatic immobilization of GOx within functionalized membrane pores, development of glucose oxidase (GOx)-horseradish peroxidase (HRP) bienzymatic system based on developed functionalized membrane pores, Glucoamylase-GOx-HRP multienzymatic system development within functionalized membrane pores and study of the reusability of the developed functionalized membrane and the phospholipid bilayer. Different approaches for membrane functionalization are also described in this section.

5.1. Characterization of small unilamellar vesicles (SUVs):

SUV solution, which was used to incorporate lipid bilayer within membrane pores, was characterized by (i) Dynamic Light Scattering (DLS), (ii) Atomic force microscopy (AFM) and (iii) Nile Red fluorescent dye [85]. Average hydrated diameter of the SUVs obtained by DLS analysis was observed to be around 90 nm as demonstrated in Figure 5.1. Point to be noted that SUV diameter of <100 nm is preferable for SLB formation [86]. Therefore, the SUVs obtained were of satisfactory quality to perform the subsequent SLB formation within the membrane pores by Vesicle-Fusion technique.

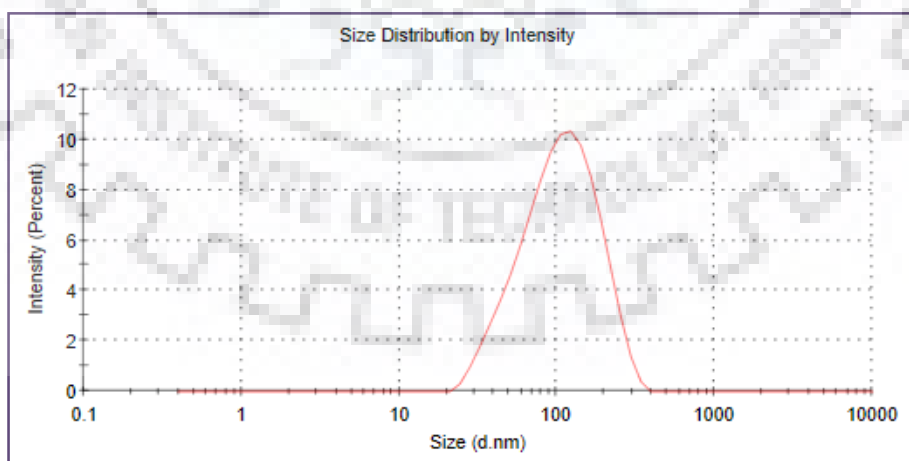


Figure 5.1. Representative DLS profile of SUVs of DMPC. DMPC concentration of SUV solution was 0.67 mg/mL in 0.1 M NaCl.

To confirm the presence of SUVs in the sample used for functionalizing membrane pores with lipid bilayer, the SUV solution was observed under AFM. The image obtained is shown in Figure 5.2, which confirms the presence of spherical SUVs in the solution.



Figure 5.2. AFM images of SUVs of DMPC. DMPC concentration was 0.67 mg/mL in 0.1 M NaCl.

Same SUV sample, which was used for DLS and AFM analysis was stained with lipid specific Nile Red fluorescent dye [85], and was observed under fluorescence microscope. The image after staining is shown in Figure 5.3, which again confirms the presence of spherical SUVs in the solution used for functionalization of membrane pores.



Figure 5.3. Nile Red fluorescence of SUVs of DMPC. DMPC concentration was 0.67 in 0.1 M NaCl, Nile Red concentration was 1 mg/mL

5.2. Functionalization of membranes and GOx immobilization:

5.2.1. Functionalization of membrane with lipid bilayer:

After preparation of desired SUV solution of DMPC, nylon membrane pores were functionalized with phospholipid bilayer, thus depositing SLB within membrane pores. Phospholipid bilayer was incorporated within nylon membranes using two different approaches. In the first approach, lipid bilayer was directly deposited within the pores of membrane and such lipid deposited membrane (L) was then used for enzyme immobilization. While in the second approach, a cushion of polymer was covalently attached within membrane pores prior to the incorporation of lipid bilayer (CL), as explained in Materials and Methods section.

The amounts of lipid deposited in L and CL membranes are presented in Table 4.1. CL was observed to have ~ 83 % higher lipid incorporation as compared to L. The spacer arm (PEI) contains numerous amine groups. Therefore, eventually, a single amine group of nylon membrane was transformed to multiple amine groups via PEI immobilization within CL membrane pores. Hence, the number of immobilization sites for phospholipid was higher with PEI spacer arm for CL than L, which was also evident by the higher phospholipid content within CL membrane pores

than the pores of L membrane. Covalently attached polymer cushion of CL provided a highly stable and soft hydrated space between the lipid bilayer and the pore surface of the membrane by several nanometers in contrast to L, where only $\sim 10\text{--}20$ Å thin water layer was present [46]. This increased space reduced the friction between the pore surface and the lipid bilayer, thereby ensuring the formation of structurally stable lipid bilayer with better mobility in CL as compared to L. Several reported studies, such as Wong et al. (1999), have also emphasized the importance of finding a suitable support material that maintains the structural and dynamic integrity of the immobilized lipid bilayer [84]. It is evident from the above result that CL functioned as a better support material than L for incorporating lipid bilayer. The long chain PEI molecules also provided an extended platform for lipid bilayer incorporation with significantly higher pore coverage for CL as compared to L.

Table 5.1. Amount of lipid deposited and amount of GOx immobilized within the pores of bare nylon membrane (B), lipid deposited nylon membrane (L) and lipid deposited with cushion polymer on nylon membrane (CL). (Conditions: pore size of bare nylon membrane $0.2\ \mu\text{m}$, external membrane area $4.9\ \text{cm}^2$ and membrane thickness $160\ \mu\text{m}$)

Membrane type	DMPC (μg)	DMPC ($\mu\text{g}/\text{cm}^2$)	GOx (μg)	GOx ($\mu\text{g}/\text{cm}^2$)
B	-	-	64.0 ± 2.2	13.1 ± 0.4
L	537.6 ± 2.1	109.7 ± 0.4	326.0 ± 2.4	66.5 ± 0.5
CL	983.2 ± 1.9	200.6 ± 0.4	700.0 ± 2.8	142.8 ± 0.6

In order to study the significance of pores for lipid bilayer functionalization compare to membrane surface, phospholipid bilayer was deposited on membrane surface by soaking mode as explained in Materials and Methods section. Point to be noted that lipid attachment only on the

surface of the L and CL membranes was found to be negligible compared to the attachment within pores. Soaking mode lipid deposition resulted in attachment of only 5 μg and 9 μg of DMPC for L and CL, respectively, whereas convective flow mode for lipid deposition within pores resulted into 537 μg and 983 μg of DMPC for L and CL, respectively. This ~ 100 folds enhanced lipid incorporation for pores as compared to surface was because of the higher surface area of the pores over the external surface of the membrane. The comparison of the internal surface area to the external surface area of a membrane is governed by the following equation [87]:

$$R = 2N\pi r_p L / [N\pi r_p^2 (1-\varepsilon)\varepsilon^{-1}] = [L/r_p][\varepsilon/(1-\varepsilon)]$$

Where, R is the ratio of the internal surface area to the external surface area of a membrane, N is the number of pores, r_p is the membrane pore radius, L is the membrane thickness, and ε is the membrane porosity. R was calculated to be ~ 3733 , i.e. accessible surface area of membrane pores was more than 3500-fold higher as compared to the external membrane surface.

5.2.2. Immobilization of glucose oxidase (GOx):

GOx, as a model enzyme, was immobilized within the pores of L, CL and within the pores of bare nylon membrane (B). The quantification of immobilized GOx revealed that both L ($326.0 \pm 2.4 \mu\text{g}$ or $67.0 \pm 0.5 \mu\text{g}/\text{cm}^2$) and CL ($700.0 \pm 2.8 \mu\text{g}$ or $143.0 \pm 0.6 \mu\text{g}/\text{cm}^2$) had almost 5 and 11 folds higher loading capacity, respectively, as compared to the loading capacity of B ($64.0 \pm 2.2 \mu\text{g}$ or $13.0 \pm 0.4 \mu\text{g}/\text{cm}^2$) as demonstrated in Table 4.1. This result can be accredited to the extended framework of the functionalized moieties within the pores of L and CL, which had increased the available effective area for GOx immobilization as compared to B. Almost 2 times higher enzyme loading in CL as compared to L can be correlated to the lipid bilayer formation on extended cushion of polymers within pores of CL. Higher amount of incorporated lipid in CL offered higher surface area for GOx loading as compared to L.

In each step of functionalization, various functionalities (PEI, phospholipid bilayer and GOx) were incorporated within membrane matrix that occupied a fraction of pore area and offered resistance to the transport through membrane pore. However, since the incorporated functional architectures were porous and hydrophilic, overall reduction in water permeability after GOx immobilization was less than 15 % of the water permeability of the bare membrane. So, the functionalization did not significantly affect the transport characteristics of the system, but

provided significant benefits in terms of activity, stability and operating range of pH as discussed further.

5.2.3. Activity of immobilized GOx:

Glucose and oxygen react in presence of GOx to form gluconic acid and hydrogen peroxide (H_2O_2). To determine the activity of immobilized GOx, the production of H_2O_2 ($\mu M H_2O_2/\mu g GOx$) within the pores of B, L and CL membranes was measured for a fixed glucose concentration (15 mM) and flow rate (2 mL/min). Figure 5.4 demonstrates that GOx, in all three immobilized forms, was capable of maintaining constant H_2O_2 production over a period of 30 min as expected for a continuous steady state reactor. This reveals the stable nature of the immobilized GOx in all three forms that were not affected by the product inhibition or other causes of enzyme deactivation as generally observed for GOx in free form [88]. Constant product formation (activity) for longer duration is very important for bioprocess industries in order to maintain the desired productivity. In present study, the lipid bilayer functionalized membranes (L and CL) were used to demonstrate that capability for 30 min.

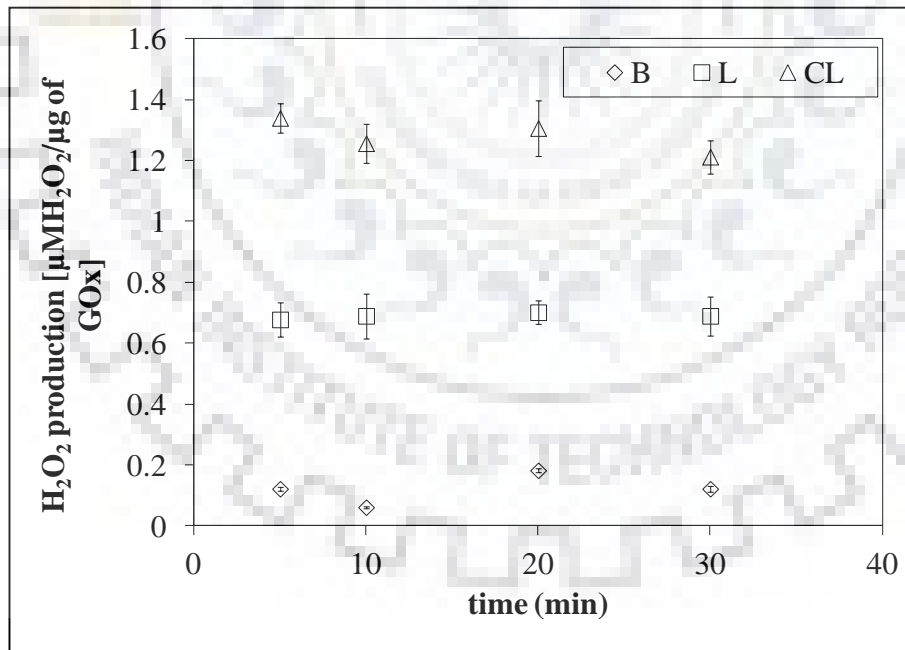


Figure 5.4 Activity study of immobilized GOx within pores of B (Bare nylon membrane), L (Lipid deposited membrane) and CL (Polymer cushioned lipid deposited membrane). Errors bars shown are in standard deviation.(Conditions: Flow rate 2 mL/min, substrate concentration 15 mM, pH 6.5)

Figure 5.4 also reveals that compare to B, L and CL membranes exhibited higher activity per unit amount of the immobilized enzyme. This was possible because of the presence of hydrated conducive environment for GOx molecules in presence of the lipid bilayer within the pores of L and CL membranes. Due to the fluidity of the lipid bilayer, enzymes were able to circumvent any possible denaturation by post-immobilization arrangement [16]. Another important observation from the activity study was that the CL membranes had higher (~ 91 %) activity than L, which can be attributed to the presence of polymer cushion prior to the lipid bilayer within CL membranes. Due to the presence of polymer cushion, the soft hydrated space between the pore surface and the lipid bilayer increased, which acted as a spacer arm to keep the active sites of the enzyme away from the pore surface. Therefore, the number of active sites of the enzyme is greater for CL compare to L. Apart from that, CL contained a lipid bilayer with better stability and mobility [84] which aided in post-immobilization arrangement of the enzyme active sites compare to L [16]. Moreover, due to the dangling functionalized architecture provided by the polymer cushion and the lipid bilayer, pore coverage of CL membrane was higher than L (where only lipid bilayer was present). Therefore, the accessibility of the immobilized active sites of GOx was better for CL than L, which led to higher activity per unit amount of immobilized enzyme ($\mu\text{M H}_2\text{O}_2/\mu\text{g GOx}$).

During the whole functionalization process, some GOx molecules got attached to the surface of the membrane as well. To understand the extent and nature of the surface immobilization of GOx, a membrane was developed with GOx immobilized primarily on the surface (by conducting the functionalization steps under soaking mode rather than convective mode). Then, a comparative study of the activity of GOx immobilized only on the surface of the membrane and GOx immobilized within the pores was done by permeating the substrate solution at convective mode under an applied pressure gradient. The concentration of H_2O_2 (μM of H_2O_2) produced by pore immobilized GOx was observed to be 98 % higher as compared to that produced by surface immobilized GOx. This was because of the insignificant immobilization of GOx on membrane surface ($6.0 \pm 0.2 \mu\text{g}$ or $1.22 \pm 0.04 \mu\text{g}/\text{cm}^2$) as compared to that within the pores ($700.0 \pm 2.8 \mu\text{g}$ or $143.0 \pm 0.6 \mu\text{g}/\text{cm}^2$). The activity [$\mu\text{M H}_2\text{O}_2/\mu\text{g GOx}$] of the pore immobilized GOx was also observed to be substantially higher than that for surface immobilized GOx as demonstrated in Figure 5.5. It is evident from Figure 5.5 that the activity of pore immobilized GOx remained constant at

around $\sim 1.3 \mu\text{M H}_2\text{O}_2/\mu\text{g GOx}$ for 30 min, whereas the same for surface immobilized GOx remained constant at around $0.63 \mu\text{M H}_2\text{O}_2/\mu\text{g GOx}$. Therefore, not only the surface had less immobilization of GOx, but the activity per unit amount of GOx (specific activity) was also lower for surface immobilized GOx compare to the pore immobilized GOx. This can be attributed to the enhanced accessibility of the immobilized GOx molecules by the substrate molecules within the pores due to the open microporous structure of the membrane. Overall, GOx immobilized in pores of CL was observed to be superior to other membranes both in terms of enzyme loading and enzyme activity. Therefore, cushioned lipid deposited membranes with pore immobilized GOx (CL) were selected for further studies.

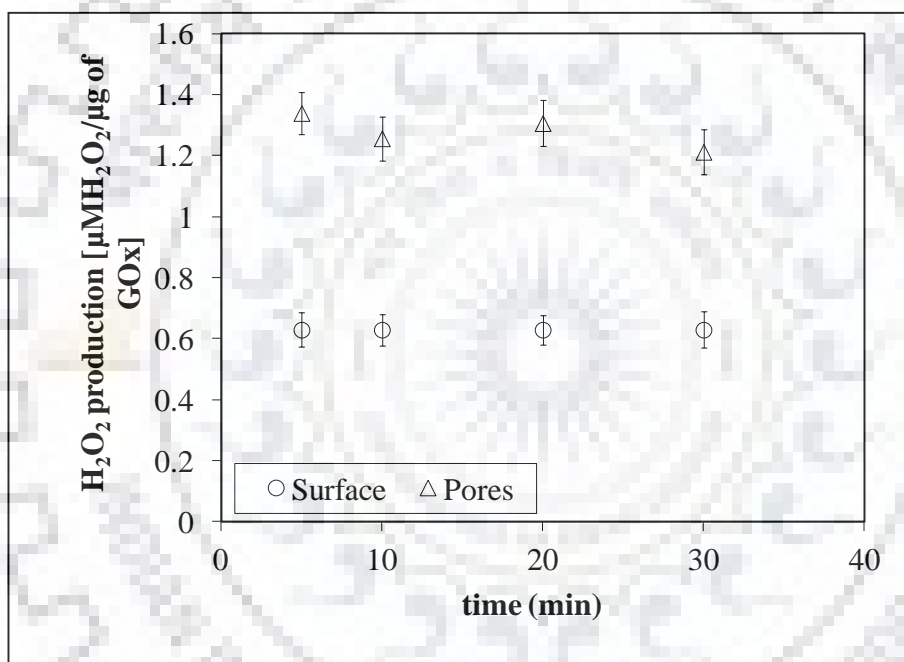


Figure 5.5. Activity study of GOx immobilized on surface and within pores of cushioned lipid deposited membranes (CL). Errors bars shown are in standard deviation. (Conditions: Flow rate 2 mL/min, substrate concentration 15 mM and pH 6.5)

5.2.4. Effect of operating conditions:

5.2.4.1. Type of flow: Effect of the type of flow on the rate of H₂O₂ production by GOx immobilized within CL membrane was investigated by performing two sets of experiments. In one set, experiments were performed with pressure driven convective flow by using a dead-end membrane holder with continuous permeation of feed solution from a reservoir. Due to this constant concentration of substrate was maintained throughout the operation. In another set, soaking mode experiments were performed to study the effect of diffusive transport. For both sets of experiments, the same GOx immobilized membrane was used. The rate of H₂O₂ production with convective mode of flow was observed to be $47.06 \pm 2.03 \mu\text{M H}_2\text{O}_2/(\mu\text{g GOx}\cdot\text{min})$ whereas, for diffusive mode of flow, rate of H₂O₂ production was $0.54 \pm 1.47 \mu\text{M H}_2\text{O}_2/(\mu\text{g GOx}\cdot\text{min})$. Convective flow offered enhanced mass transfer than diffusive flow, which led to faster transport of the components (substrates and products). The accessibility of the substrate for the enzyme was also significantly improved for the convective mode as compared to the diffusion mode [3].

5.2.4.2. Flow rate (residence time): To study the effects of residence time on H₂O₂ production and rate of H₂O₂ production by immobilized GO_x within the pores of CL membrane, flow rate was varied within the range of 0.5 mL/min to 3 mL/min. For different flow rates, residence time (τ) was calculated according to the following mathematical equation [89]:

$$\tau = V/v$$

Where, τ = Residence time, V = Porous volume = Total volume \times Porosity (ϵ), v = volumetric flow rate. Total volume = $\pi \times r^2 \times L$; r = radius of membrane, L = thickness of the membrane.

For, $r = 12.5 \text{ mm}$, $L = 160 \mu\text{m}$ and $\epsilon = 0.7$, τ was calculated to be 0.108 min, 0.054 min, 0.027 min and 0.018 min for $v = 0.5 \text{ mL/min}$, 1 mL/min , 2 mL/min and 3 mL/min , respectively.

Effects of flow rate on H₂O₂ production [$\mu\text{M H}_2\text{O}_2/\mu\text{g}$ of GOx] and rate of H₂O₂ production [$\mu\text{M H}_2\text{O}_2/\mu\text{g}$ of GOx/min] are elucidated in Figure 5.6 For a constant substrate concentration, decrease in H₂O₂ production [$\mu\text{M H}_2\text{O}_2/\mu\text{g}$ of GOx] was observed with increase in flow rate (from 0.5 mL/min to 3 mL/min). This is because with increase in flow rate, residence time decreased, due to which lesser number of substrate molecules were converted to product molecules per unit volume of solution. Figure 5.6 also shows that the rate of H₂O₂ production [μM

$\text{H}_2\text{O}_2/\mu\text{g}$ of GOx/min] increased asymptotically with increase in flow rate (i.e. with decrease in residence time). The increase in rate of H_2O_2 production with flow rate was higher for flow rate range of 0.5-2 mL/min, and then it gradually tailed off at flow rate greater than 2 mL/min. For an ideal flow reactor, such as plug flow reactor (PFR) or mixed flow reactor (MFR), in absence of mass transfer limitations, the rate of product formation should be independent of flow rate (and hence residence time) [3]. Similar trend is observed in Figure 5.6 for higher flow rate (i.e. above 2 mL/min), where mass transfer resistance was negligible and the membrane reactor approached the ideal reactor model. However, at lower flow rate (i.e. 0.5-2 mL/min), deviation from ideal reactor behavior was observed. The deviation can be attributed to the appearance of mass transfer resistance at lower flow rates. Due to mass transfer resistance, all the active sites of immobilized GOx were not accessible for glucose molecules, which in turn decreased the rate of H_2O_2 production.

In this study, the maximum rate of H_2O_2 production [μM $\text{H}_2\text{O}_2/\mu\text{g}$ of GOx/min] was observed to be 47 μM $\text{H}_2\text{O}_2/\mu\text{g}$ of GOx/min corresponding to a flow rate of 2 mL/min (residence time of 0.027 s). The activity of electrostatically immobilized GOx within functionalized PVDF membrane pores was reported to be 17 μM $\text{H}_2\text{O}_2/\mu\text{g}$ of GOx/min at a residence time of 0.6 s by Datta et al. (2008) [3]. Therefore, the phospholipid bilayer functionalized membrane pore supported by cushion of polymer exhibited significant advancement from the previously reported study.

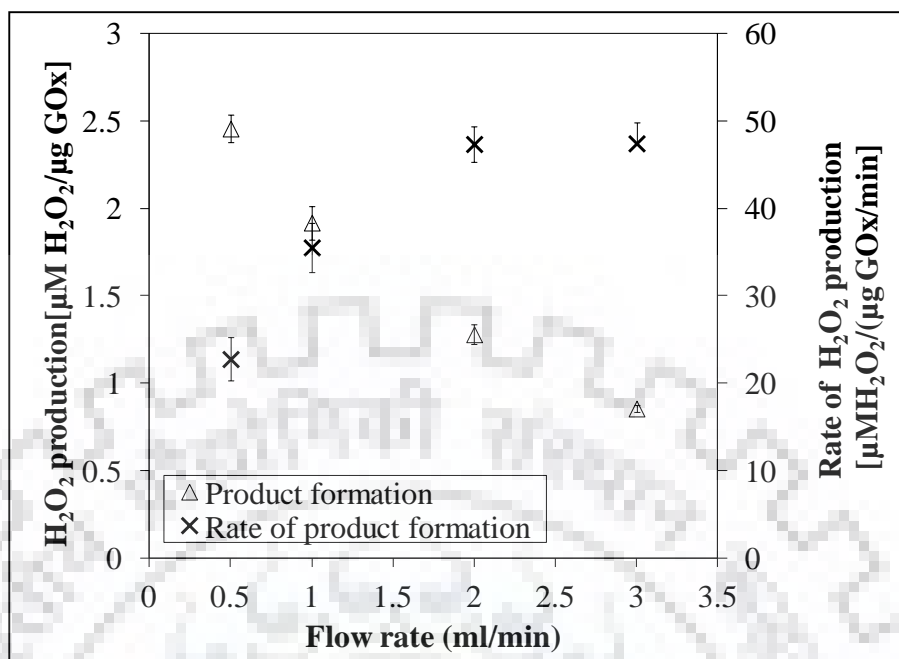


Figure 5.6. Effect of residence time (i.e. flow rate) on production of H₂O₂ and rate of H₂O₂ production for 15 mM glucose solution by GOx immobilized within the pores of CL nylon membrane. (Conditions: amount of immobilized GO_x 700 μg, pH 6.5, temperature 25 °C, and residence time 0.108 – 0.018 min).

5.2.4.3. Effect of pH: The effect of pH on the activity of free GOx and immobilized GOx (within pores of CL membranes) is represented in Figure 5.7 in terms of normalized activity. Normalization was performed on the basis of maximum activity of both free and immobilized enzyme. At pH 5.5, free GOx demonstrated maximum activity, however a drastic decrease in activity was observed on either side of pH 5.5. Similar trend in activity of free GOx has earlier been reported in literature [90–93]. On the other hand, maximum activity of immobilized GOx was observed at pH 6.5. Other studies have also reported a shift in optimum pH for maximum activity of immobilized enzyme [94–96]. The reason for this behavior was the change in the microenvironment (H⁺ and OH⁻ concentrations) of the enzyme due to the functionalization within membranes [97]. What is more important is the fact that on either side of the optimum pH of 6.5, the activity did not decrease substantially for the immobilized enzyme. For example, the immobilized GOx demonstrated normalized activity (with respect to the activity at pH 6.5) of 96 % at pH 4.5 and 81 % at pH 8 with 15 mM glucose solution. In comparison, the free GOx

demonstrated normalized activity (with respect to the activity at pH 5.5) of 63 % at pH 4.5 and 39 % at pH 8 with 15 mM glucose solution. Therefore, the range of optimum pH (pH ~ 4 to 8), where the enzyme can be operated without any substantial loss of productivity, is broader for the immobilized GOx than the free GOx. This pH tolerance of immobilized enzyme can be beneficial for applications involving wider range of pH, because of the absence of significant loss of enzyme activity.

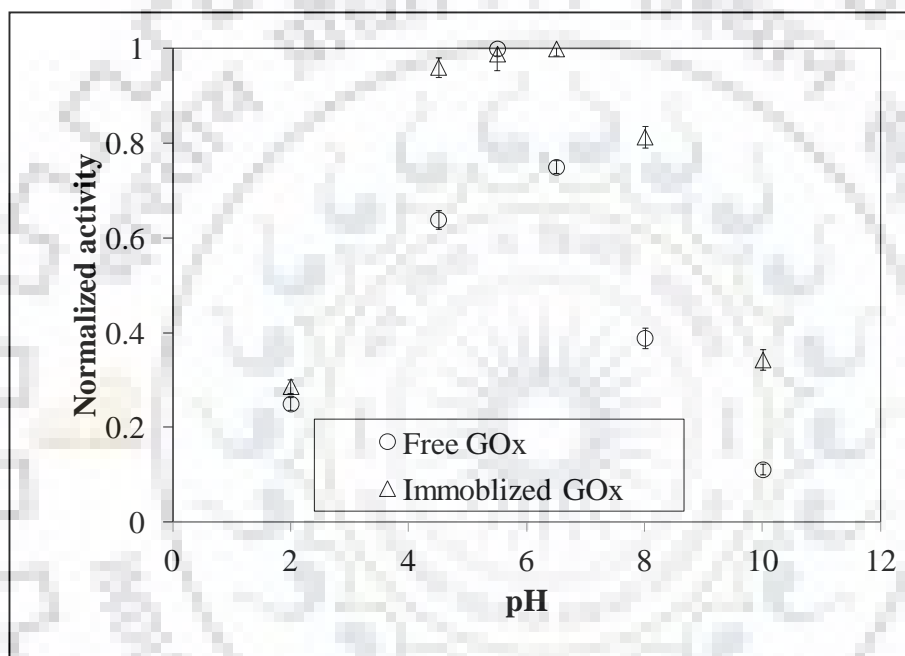


Figure 5.7. Effect of pH on activity of free GOx and GOx immobilized within pores of CL membrane. Activity was calculated based on the concentration of H_2O_2 produced and was normalized on the basis of the maximum activity. (Conditions: Maximum activity of free GOx $39 \mu M H_2O_2/\mu g$ of GOx, maximum activity of immobilized GOx $1.27 \mu M H_2O_2/\mu g$ of GOx, amount of GOx immobilized $700 \mu g$, residence time $1.62 s$, external membrane area $4.9 cm^2$, membrane thickness $160 \mu m$, temperature $25 ^\circ C$ and concentration of glucose $15 mM$).

5.2.5. Storage stability of immobilized GOx: The storage stability of the immobilized GOx within the pores of CL membrane was monitored and compared with free GOx by measuring the

change in activity for 28 days. The activity of immobilized GOx and free GOx was analyzed by flow-through mode and batch mode, respectively. The comparison of the activity was done by normalizing each activity with respect to the maximum activity. For both immobilized and free GOx, the maximum activity was observed on the first day. As depicted in Figure 5.8, immobilized GOx retained 85 % of its initial activity, whereas free GOx retained only 22 % of its initial activity after 28 days of storage. In literature, the activity of free GOx has been reported to be reduced to 25 % after 28 days [98] and to 30 % after 7 days [91]. This indicates that the pores of CL membrane provided better protection to GOx compare to free GOx, thereby, helping the latter one to retain its activity over longer period of time. The stability study further highlights the importance of immobilized enzymes for long term industrial applications and confirms the ability of the lipid bilayer functionalized membrane to achieve the same.

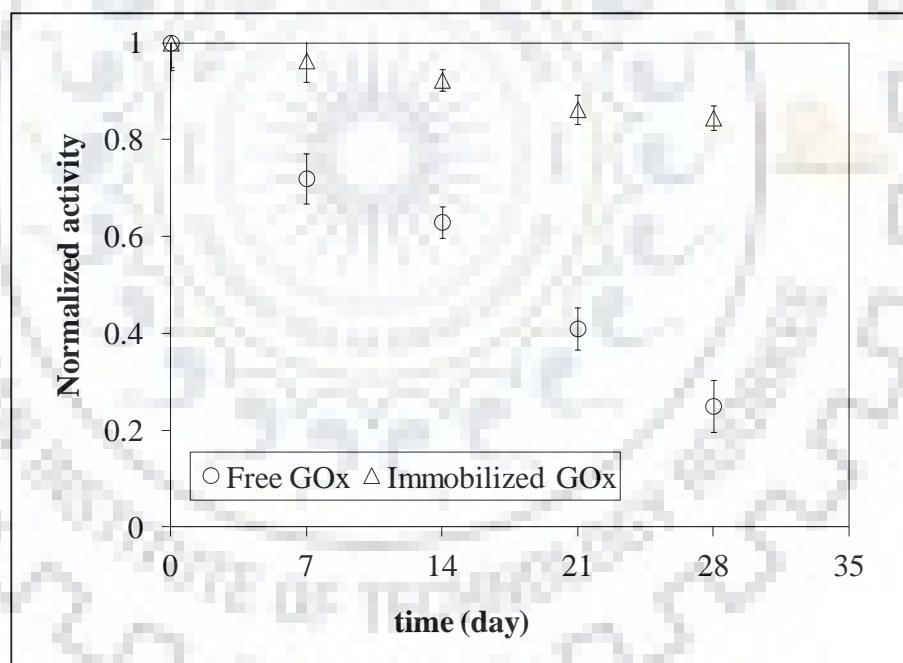


Figure 5.8. Storage stability of free GOx and GOx immobilized within the pores of CL membrane over a period of 28 days. Activity was calculated based on the concentration of H_2O_2 and was normalized by dividing with the activity on the first day.

Since, phospholipid bilayer functionalized membrane pores were developed and examined for enzymatic catalysis by electrostatically immobilizing glucose oxidase (GOx) as model enzyme, further experiments were conducted to investigate the use of developed functionalized membrane for electrostatic immobilization of another enzyme containing opposite charge of previously immobilized GOx. This was followed by electrostatic co-immobilization of two enzymes containing opposite charges, GOx and HRP, within phospholipid bilayer functionalized membrane pores to develop a novel bienzymatic system based on SLB functionalized nylon membrane pores.

5.3. Immobilized glucose oxidase (GOx)-horseradish peroxidase (HRP) bienzymatic system:

5.3.1. Immobilization of GOx and HRP enzymes:

To study the loading of the individual GOx and HRP enzymes, they were separately immobilized within the pores of B, L and CL membranes. To prepare GOx-HRP bienzymatic system, GOx and HRP enzymes were co-immobilized within the same CL membrane (CL-C). For co-immobilization, the negatively charged GOx molecules (pI-4.2) [99] were first electrostatically bound to the positively charged amine-groups at pH 6.5. Then, at pH 6.5, the positively charged HRP molecules (pI-8.8) [100] were electrostatically bound to the negatively charged phosphate groups of zwitterionic DMPC (Figure 5.9). The results of enzyme loading for different cases are represented in Figure 5.10.

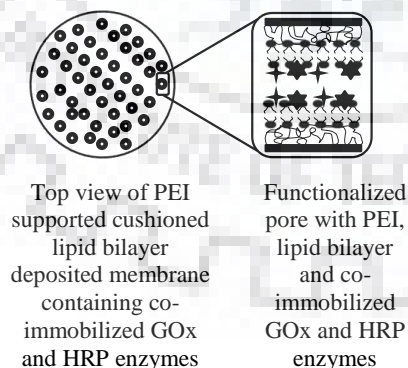


Figure 5.9. Co-immobilization of GOx (★) and HRP (✦) enzymes within CL membrane.

Quantification of GOx revealed that in comparison to B, both L and CL had higher (5-fold and 11-fold, respectively) enzyme loading. Similarly, HRP immobilization was also found to be higher for L and CL (4.3 fold and 11.6-fold, respectively) as compare to B. Co-immobilized GOx and HRP within the same CL membrane (CL-C) had similar amount of immobilized enzymes as were for separate membranes (CL). The observation of higher HRP loading within the pores of L and CL membranes in comparison to B is consistent with our earlier explanation for GOx [101] (Section 4.2.2), which suggested that the extended framework of the functionalized moieties had increased the available effective area within the pores for L and CL membranes for enzyme immobilization as compare to B.

5.3.2. Study of the activity of immobilized HRP enzyme: Activity of immobilized HRP enzyme was determined by using ABTS as a chromogen. Two molecules of ABTS react with one molecule of H₂O₂ producing two molecules of ABTS^{•+} in the presence of HRP enzyme. The concentration of the product ABTS^{•+} was monitored to determine the activity of immobilized HRP. The production of ABTS^{•+}, i.e. the activity of immobilized HRP under convective flow ($\mu\text{M ABTS}^{\bullet+}/\mu\text{g HRP}$), within the pores of B, L and CL membranes was measured for fixed concentrations of ABTS (3 mM) and H₂O₂ (1.3 mM) supplied as substrates.

Figure 5.10 demonstrates that HRP activity was higher for both L and CL membranes as compare to B. L membrane was observed to have 6-fold higher activity of HRP in comparison to HRP activity in B membrane. This was possible because biomimetic lipid bilayer provided a conducive native cell-like environment for HRP molecules. The fluidity of the lipid bilayer allowed enzymes to circumvent any possible denaturation by undergoing post-immobilization rearrangement [16].

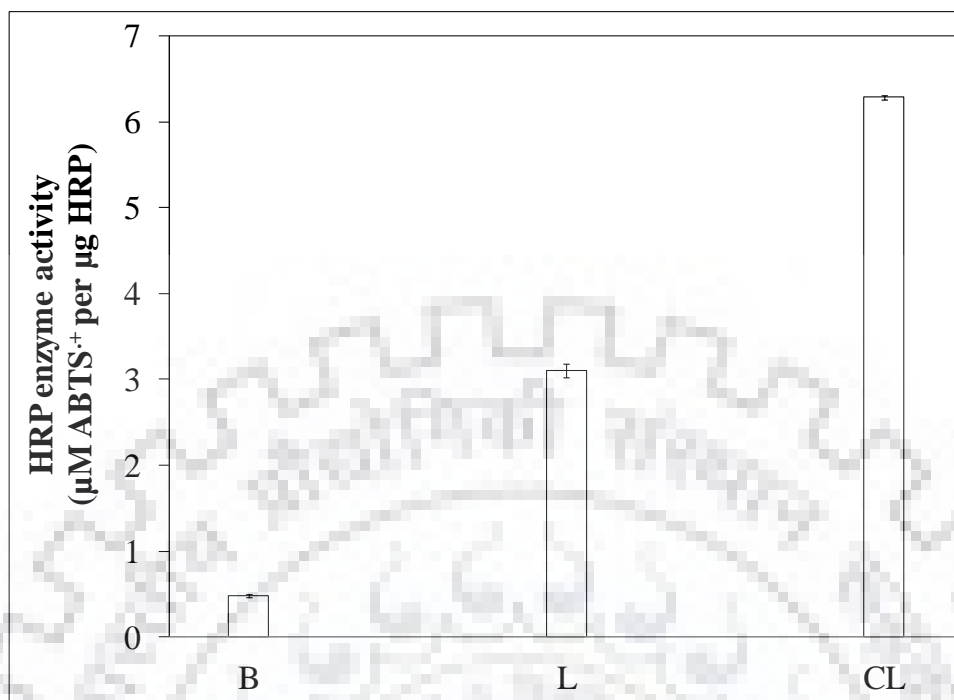


Figure 5.10 Activity of immobilized HRP enzyme within pores of B, L and CL membranes. Data points are represented by the mean \pm standard deviation for $n=3$. (Conditions: Flow rate 2 mL/min, ABTS concentration 3 mM, H_2O_2 concentration 1.3 mM, pH 6.5)

The activity study also revealed that the CL membranes had significantly higher HRP activity than L (~2 folds higher activity, p -value < 0.05). This can be attributed to the presence of polymer cushion prior to the lipid bilayer within CL membranes. The presence of polymer cushion increased the soft hydrated space between the membrane pore surface and lipid bilayer. This increased hydrated space acted as a spacer arm to keep the active sites of the enzyme away from the pore surface. Consequently, the number of available catalytic active sites per unit amount of the enzyme was greater for CL as compared to L. Apart from that, more stable and mobile lipid bilayer in CL [84] aided in post-immobilization rearrangement of the enzyme active sites compare to L [16]. Moreover, the dangling functionalized architecture, provided by the polymer cushion increased the pore coverage of CL membrane than L (where only lipid bilayer was present). As a result, the accessibility of the catalytic active sites of immobilized HRP molecules was better for CL than L, which resulted into higher activity per unit amount of immobilized enzyme ($\mu\text{M ABTS}^{*+}/\mu\text{g HRP}$). In previous section (4.2.3), similar observation is reported for GOx enzyme.

The investigation of amount of immobilized GOx and HRP enzymes revealed that CL membranes had higher enzyme loading than L and B membranes. The activity study of immobilized HRP enzymes demonstrated higher activity for CL membrane than L and B membranes. Co-immobilization of GOx and HRP enzymes within CL membrane exhibited similar enzyme loading as obtained for individual GOx and HRP enzyme immobilization within separate CL membranes. Hence, it can be concluded that CL membrane was superior to other membranes both in terms of enzyme loading and enzyme activity. Therefore, CL membrane was selected for further studies to develop GOx-HRP bienzymatic system.

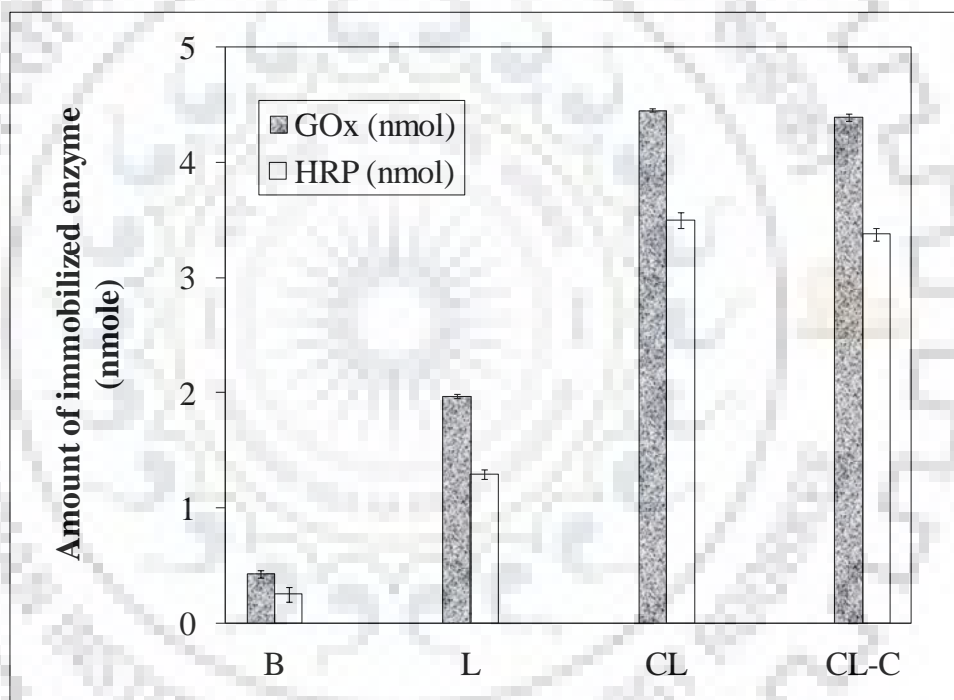


Figure 5.11. Amount of immobilized GOx and HRP within B (blank), L (lipid bilayer deposited) and CL (polymer cushion supported lipid bilayer attached) membrane pores. CL-C represents co-immobilized GOx and HRP enzymes within the same CL membrane. Data points are represented by the mean \pm standard deviation for $n=3$. (Conditions: Flow rate 2 mL/min, pH 6.5)

Similar amount of immobilized GOx and HRP for separate CL and same (CL-C) membrane can be attributed to the presence of same amount of negatively charged phosphate groups and positively charged amine-groups on DMPC of CL and CL-C. Figure 5.11 also reveals

lower amount of immobilized HRP compare to GOx for all four cases. For B membrane, since nylon membrane has slight positive charge, environment for attachment of negatively charged GOx was more conducive than positively charged HRP. In case of L and CL membranes, negative charged phosphate groups of lower layer of lipid bilayer was occupied interacting with positive amine groups of nylon membrane and PEI matrix, respectively. Therefore, phosphate groups of only upper layer of lipid bilayer were available for positively charged HRP molecules. Whereas, positive amine groups of both upper and lower layers of lipid bilayer interacted with negatively charged GOx molecules resulting into higher amount of GOx loading than HRP. Additionally, lower amount of HRP loading than GOx in CL membrane could also be attributed to the repulsive force between the positively charged HRP molecules and amine groups of polymer cushion.

5.3.3. Activity of the immobilized GOx-HRP bienzymatic system: The activity of the immobilized GOx-HRP bienzymatic system was studied for two configurations of CL membrane. First configuration consisted of two different CL membranes, containing individual enzymes, placed one above the other during the activity analysis study of bienzymatic system. The top CL membrane had electrostatically immobilized GOx enzyme and the bottom CL membrane contained electrostatically immobilized HRP enzyme. This configuration will be referred as stack configuration or CL-S in further text. Second configuration, containing both GOx and HRP electrostatically immobilized within the same CL membrane, will be referred as co-immobilized configuration or CL-C in further text.

Initially, only glucose (15 mM) solution was passed through both CL-S and CL-C configurations at 2 mL/min. The concentration of H₂O₂ produced internally (by immobilized GOx) was observed to be 1.3 mM for both of the configurations. Since the stoichiometric ratio between H₂O₂ and ABTS is 1:2 for the formation of ABTS^{•+} [102], the concentration of ABTS in feed solution for both CL-S and CL-C configurations was maintained at 3 mM for further experiments. The concentration of ABTS was kept more than twice to ensure the reaction is not limited by ABTS. The activity for both of the configurations was determined by permeating a feed solution containing 15 mM glucose (saturated with O₂) and 3 mM ABTS. For the CL-S configuration, glucose was oxidized by GOx present in the top membrane to produce H₂O₂ and gluconic acid. Produced H₂O₂, then, reached the bottom membrane containing HRP enzyme and oxidized ABTS in presence of HRP to form ABTS^{•+} [102]. However, in CL-C configuration, both

of the steps of H_2O_2 and ABTS^{++} production occurred successively within the same CL membrane. The activity of both configurations (CL-S and CL-C) was calculated in terms of $\mu\text{M ABTS}^{++}$ produced per μg of immobilized HRP.

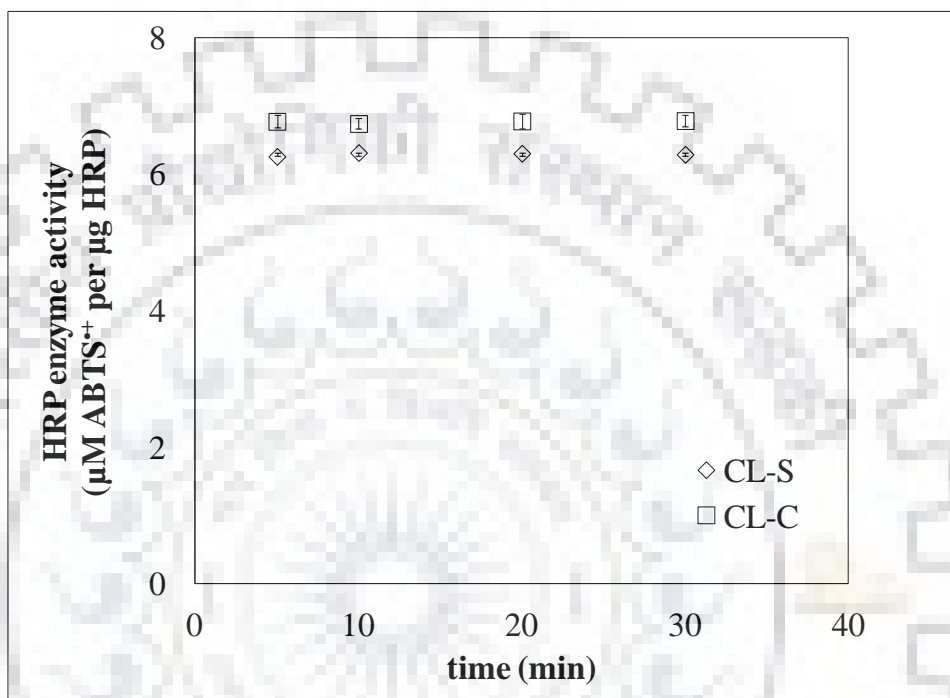


Figure 5.12. Activity of CL-S and CL-C bienzymatic systems. Enzymes were immobilized within the pores of CL membrane. Data points are represented by the mean \pm standard deviation for $n=3$. (Conditions: Flow rate 2 mL/min, glucose concentration 15 mM, ABTS 3 mM, pH 6.5)

Constant ABTS^{++} production was observed for 30 min for CL-S as well as CL-C membranes as demonstrated in Figure 5.12. Constant conversion of the substrate to product is a characteristic of continuous steady state reactor [3]. Figure 5.12 also reveals that CL-C exhibited significantly higher activity (p -value < 0.05) as compare to CL-S. This can be attributed to the enhanced accessibility of the immobilized HRP molecules by the internally produced H_2O_2 molecules within the pores of the CL-C membrane. For CL-C, due to the proximity of the GOx and HRP enzymes, H_2O_2 produced within the membrane was readily available for HRP catalysis resulting into higher activity. On the other hand, for CL-S, H_2O_2 produced in the top membrane was transported to the bottom membrane,

and then participated in HRP catalysis resulting into lesser activity. In literature, there are various studies, which have reported that the overall reaction rate increased when the distance between GOx and HRP was reduced [103,104].

To compare the efficacy of CL-S and CL-C bienzymatic systems, both configurations were also investigated for the internally produced H₂O₂ utilization efficiency. Since, the theoretical stoichiometric ratio between the two reactants, H₂O₂ and ABTS, is 1:2, it was expected that 1 mole of H₂O₂ produced in presence of GOx will react with 2 moles of ABTS in presence of HRP to produce 2 moles of ABTS^{•+}. Therefore, H₂O₂ utilization efficiency for both of the systems (CL-S and CL-C) was calculated in terms of moles of H₂O₂ utilized per 2 moles of ABTS^{•+} production. The H₂O₂ utilization efficiency of CL-C and CL-S was calculated to be 76 % and 70 %, respectively. This significantly higher (*p-value* < 0.05) H₂O₂ utilization efficiency for CL-C as compared to CL-S can be attributed to the better transport characteristics of substrate molecules in CL-C system due to the proximity of the two enzymes. 70 % H₂O₂ utilization efficiency indicates the efficiency of the membrane immobilized bienzymatic system in performing a two-step series reaction under continuous flow of substrates. All these studies clearly indicate that CL-C GOx-HRP bienzymatic system has better catalytic activity than CL-S system.

5.3.4 Operating range of pH for bienzymatic system: The effect of pH on the activity of both bienzymatic configurations, CL-S and CL-C, was studied in the pH range of 4 to 9 and compared with the effect of pH on the activity of free enzymes. The activities were compared in terms of normalized form, which was calculated on the basis of maximum activity for each case.

Various studies have reported that free GOx exhibited maximum activity at pH 5.5 with a drastic decrease in activity on either side of pH 5.5 [91,93]. We also observed similar trend while studying the effect of pH on activity of free GOx in our previous section. The effect of pH on the activity of free HRP was investigated and the maximum activity was observed to be at pH 7. However, on either side of pH 7, a steep decrease in activity was observed as demonstrated in Figure 5.13. This is in agreement with the other literature reports [105,106].

The most important observation regarding the effect of pH on immobilized bienzymatic system was that within the range of pH from 5 to 9 the activity did not change substantially as represented in Figure 5.13. CL-S demonstrated normalized activity (with respect to the activity at

pH 5) of 94 % at pH 6, 90 % at pH 7, 86 % at pH 8 and 81 % at pH 9, while CL-C exhibited normalized activity (with respect to the activity at pH 5) of 96 % at pH 6, 93 % at pH 7, 90 % at pH 8 and 86 % at pH 9 with 3 mM ABTS solution. In comparison, free HRP demonstrated normalized activity (with respect to the activity at pH 7) of 57 % at pH 8 and 42 % at pH 9 with 3 mM ABTS solution. The expansion of pH dependent activity profile after immobilization has also been reported in various studies [3,107], which support the stability of the developed bienzymatic system over a broad pH-range of ~5-9. Therefore, the range of optimum pH (pH ~ 5 to 9), where bienzymatic systems can be operated without any substantial loss of productivity, was broader for both CL-S and CL-C, than free enzymes.

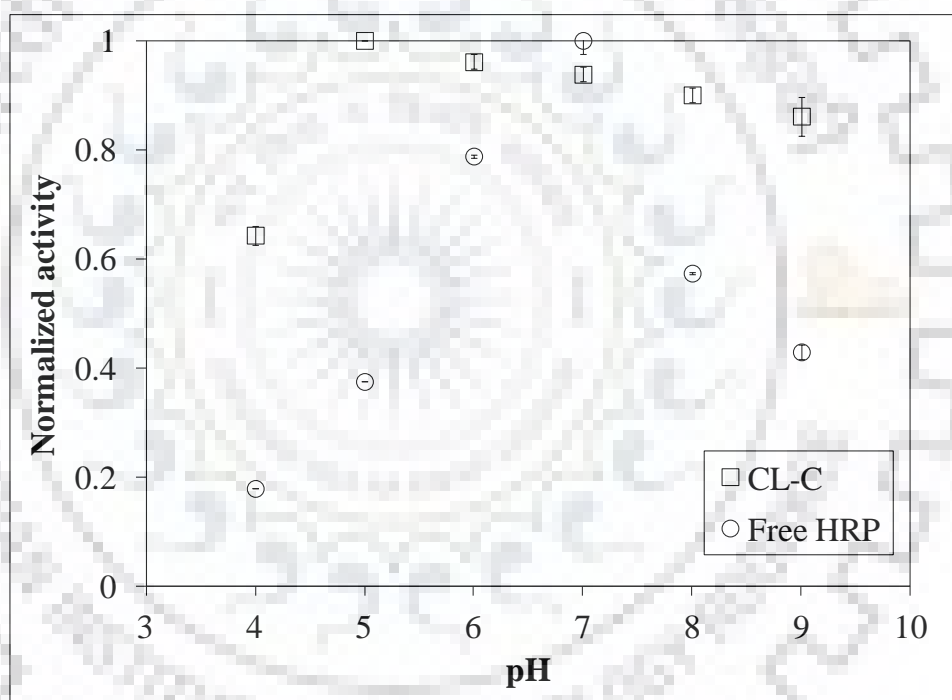


Figure 5.13. Effect of pH on activity of free enzymes and CL-C configuration. Activity was normalized on the basis of the maximum activity. Data points are represented by the mean \pm standard deviation for $n=6$ (Conditions: External membrane area 4.9 cm², thickness of one membrane 160 μ m, concentration of glucose 15 mM, concentration of ABTS 3 mM).

Both immobilized bienzymatic configurations, CL-S and CL-C, exhibited maximum activity at pH 5 (Figure 5.13). In literature, there are various studies, where a

shift in optimum pH for maximum activity was observed after simultaneous immobilization of two or multiple enzymes [107,108]. The reason for this behavior can be attributed to the change in the microenvironment (H^+ and OH^- concentrations) of the enzyme due to functionalization within membrane pores [97]. Moreover, with the shift in pH towards acidic side, PEI-matrix within the membrane pores expanded due to the repulsive interaction between the like charges [109]. This expansion increased the effective pore coverage of the functionalized moieties within membranes pores. Due to which, the accessibility of immobilized enzymes for substrate molecules increased. This increased accessibility between substrate and immobilized enzymes resulted into increased activity at acidic pH.

At pH 4, the normalized activities of CL-S and CL-C were observed to be 57 % and 63 %, respectively as compare to the normalized activity of 100 % at pH 5. This decrease in activity at pH 4 was due to the effect of low pH on immobilization of GOx. Since, the pI of GOx is 4.2, at an operating pH of 4, the net charge on GOx became positive rather than negative at a pH greater than the pI. This shift in charge of GOx affected the electrostatic interaction between the GOx molecules and the positively charged amine groups of phospholipid moieties resulting into decrease in activity and possible detachment from the functionalized matrix.

5.3.5. Storage stability of GOx-HRP bienzymatic system: The storage stability of the developed bienzymatic configurations, CL-S and CL-C, was monitored and compared with that of free enzymes by measuring the change in activity for 28 days. The comparison of the activity was done by normalizing each activity with respect to the maximum activity. For both immobilized systems as well as for free enzymes, the maximum activity was observed on the first day. As depicted in Figure 5.14, both CL-S and CL-C retained 80 % of its initial activity, whereas free HRP was observed to retain only 10 % of its initial activity after 28 days. This observation is in good agreement to previous studies dealing with the activity of free GOx [110]. This observation indicates that the pores of CL membrane provided better protection to GOx-HRP bienzymatic system compare to free enzymes, thereby, helping immobilized bienzymatic systems to retain its activity over longer period of time. The stability study further highlights the importance of immobilized enzymes for long term industrial applications and confirms the ability of the lipid bilayer functionalized membrane to achieve the same.

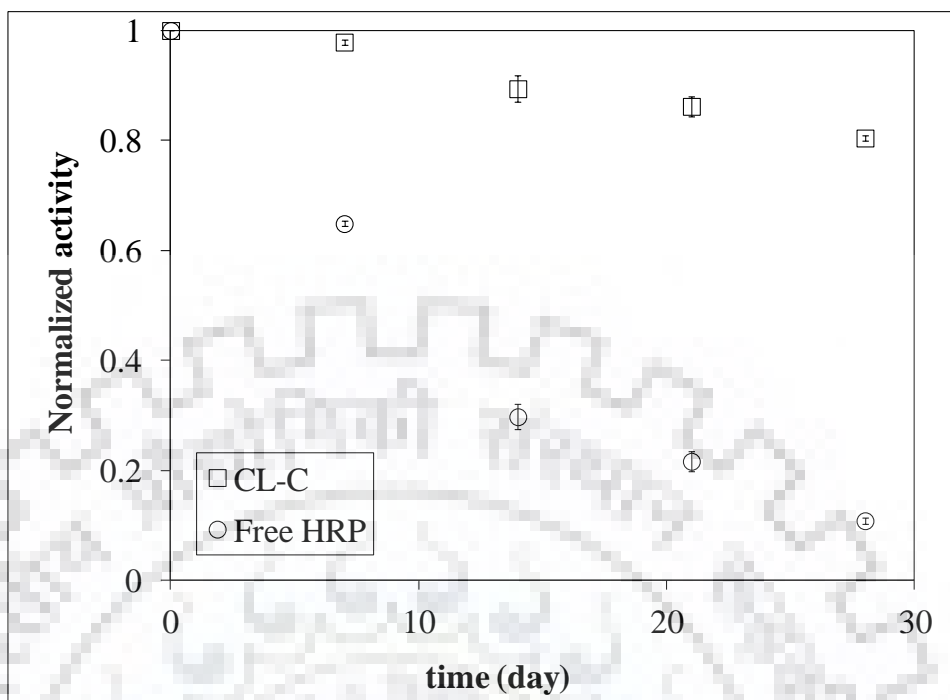


Figure 5.14. Stability of free enzymes and immobilized GOx-HRP within the pores of CL membrane over a period of 28 days. Activity was calculated and normalized by dividing with the activity on the first day.

Application of SLB functionalized nylon membrane pores for development of GOx-HRP bienzymatic system demonstrated that such SLB functionalized nylon membrane pores can be used for electrostatic immobilization of either positive or negative charged enzyme molecules. The major observation was that two enzymes containing opposite charges can be electrostatically coimmobilized with zwitterionic DMPC molecules of SLB to give better activity and satisfying storage stability along with a broader range of operating pH. This finding was further extended to investigate the possibility of development of multienzymatic system.

5.4. Immobilization and activity of GA-GOx-HRP multienzymatic system:

Phospholipid bilayer functionalized membrane was further used to develop GA-GOx-HRP based multienzymatic system. All three enzymes were immobilized electrostatically within biomimetic membrane pores. Earlier, CL membrane was observed to be superior to B and L membranes both in terms of enzyme loading and enzyme activity (section 4.2.2 and 4.2.3), and, CL-C was

demonstrated to give enhanced bienzymatic activity as compare to CL-S membrane (section 4.3.3). Hence, CL membrane was selected to develop GA-GOx-HRP multienzymatic system. GOx-HRP enzymes were coimmobilized within a membrane, whereas GA was immobilized within a separate membrane. Both of these membranes were used in stack configuration, with the GA-membrane on top of the GOx-HRP membrane, for activity analysis of multienzymatic system.

5.4.1. Immobilization of the enzymes: Although loading of GOx and HRP was studied earlier, while developing the GA-GOx-HRP multienzymatic system, loading of the individual enzymes were studied again within the pores of CL membranes.

To develop multienzymatic system, GA was immobilized within one CL membrane and GOx-HRP enzymes were coimmobilized within another CL membrane (Figure 5.15) Both these membranes were then used in stack for further studies.

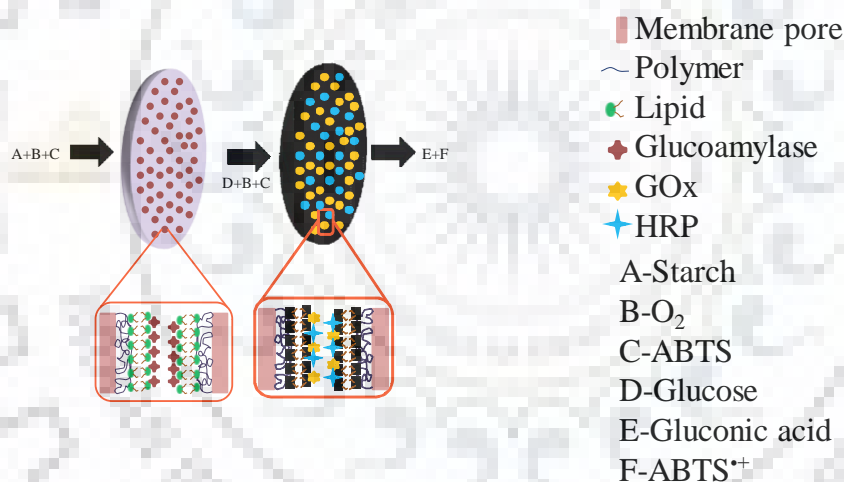


Figure 5.15 Schematic representation of multienzymatic system

At pH 6.5, the negatively charged GA molecules (pI 4.5) were electrostatically bound to the positively charged amine-groups of DMPC molecules. In case of co-immobilized GOx-HRP, the negatively charged GOx molecules (pI-4.2) and the positively charged HRP molecules (pI-8.8) were electrostatically bound to the positively charged amine-groups and the negatively charged phosphate groups of zwitterionic DMPC, respectively, at pH 6.5. The results of enzyme loading for different cases are represented in Table 4.2. For comparison, same enzymes were also

immobilized within blank nylon membranes and ~ 10-fold higher amount of enzymes were observed to be immobilized within CL membrane pores. The extended framework of the functionalized moieties within the pores of CL had increased the available effective area for immobilization of enzymes, as compare to B. This observation is consistent to our previous observation as mentioned in section 4.2.2.

Table 5.2 Amount of immobilized enzyme (nmol). B: Blank membrane, CL: Functionalized membrane with cushioned phospholipid bilayer, GOx and HRP enzymes were co-immobilized within same CL membrane

Type of Membrane	Glucoamylase	GOx	HRP
B	0.48	0.43	0.34
CL	5	4.5	3.5

5.4.2 Activity of immobilized GA-GOx-HRP multienzymatic system: Activity of GA-GOx-HRP multienzymatic system was determined by using ABTS as a chromogen. When a feed solution containing starch and ABTS (and saturated with oxygen) was passed through the stacked multienzymatic system, the following sequence of events occurred. Starch was catalytically hydrolysed to form glucose by GA. Glucose, thus produced, reacted with oxygen in presence of GOx to form H₂O₂ and gluconic acid. Then, each molecule of H₂O₂ reacted with two molecules of ABTS producing two molecules of ABTS^{•+} in the presence of HRP enzyme. The concentration of the product ABTS^{•+} was monitored to determine the activity of the multienzymatic system.

Figure 5.16 demonstrates the activity of GA-GOx-HRP multienzymatic system in terms of HRP activity. An operational stability for 30 minute was exhibited, which shows the constant rate of product formation from the substrates and conducive environment of biomimetic lipid bilayer for all three types of enzymes.

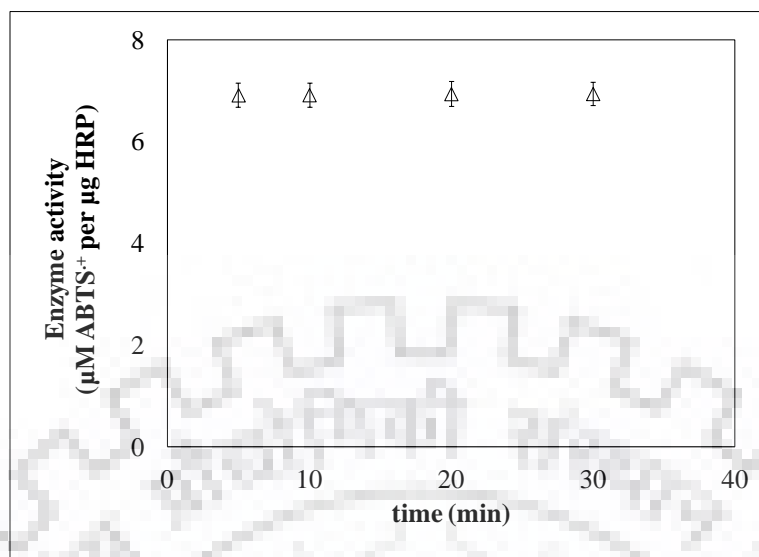


Figure 5.16 Activity of multienzymatic system containing immobilized GA and coimmobilized GOx+HRP enzymes within CL membrane. (Conditions: Flow rate 2 mL/min, ABTS concentration 3 mM, H₂O₂ concentration 1.3 mM, pH 6.5)

5.4.3. Operating range of pH for multienzymatic system:

The effect of pH on the activity of multienzymatic system was studied in the pH range of 4 to 9 and compared with the effect of pH on the activity of free enzymes. The effect of pH on the activity of GOx and HRP enzymes has already been discussed in sections 4.2.4.3 and 4.3.4. The study of the effect of pH on the activity of GA revealed that maximum activity of free as well as immobilized glucoamylase was observed at pH 5 with a steep decrease in activity on either side (Figure 5.17) Similar observation was reported in various previous literature studies [111]

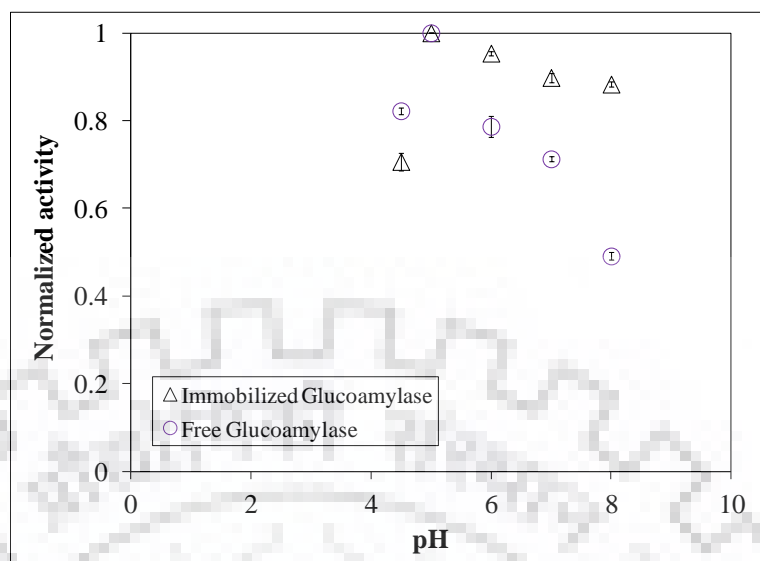


Figure 5.17. Activity of free and immobilized GA within CL membrane at different pH

The most important observation regarding the effect of pH on immobilized multienzymatic system was that within the range of pH from 5 to 9 the activity did not change substantially. The expansion of pH dependent activity profile after immobilization has also been reported in various studies [3,107], which support the stability of the developed multienzymatic system over a broad pH-range of ~5-9. Therefore, the range of optimum pH (pH ~ 5 to 9), where multienzymatic systems can be operated without any substantial loss of productivity, is broader for immobilized system than free enzymes.

5.4.4. Storage stability of multienzymatic system:

The change in activity of all three enzymes, GA GOx and HRP, was studied for 28 days and compared with that of free enzymes. The storage stability of GOx and bienzymatic system has already been discussed in sections 4.2.5 and 4.3.5, respectively. The study of activity over 28 days for immobilized GA revealed that the maximum activity was observed on the first day for both immobilized GA well as for free enzymes, as represented in Figure 5.18 The activity was observed to be reduced to 10 % on 28th day from 80 % as was observed on first day as compare to free enzymes. This observation can be attributed to the protective environment provided to immobilized GA by functionalized moieties.

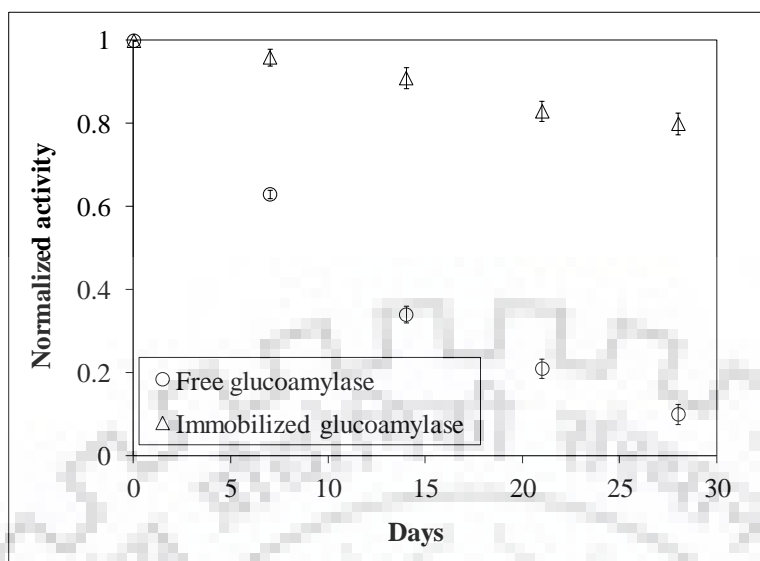


Figure 5.18 Stability of free and immobilized GA within the pores of CL membrane over a period of 28 days. Activity was calculated and normalized by dividing with the activity on the first day.

The long term stability of immobilized GA is a favorable property for industrial applications and thereby proves the importance of lipid bilayer to retain the desired stability.

Results so far obtained and discussed proves that developed novel SLB functionalized nylon membrane pores can be successfully used for single, bi- or multienzymatic systems and all these systems are quite stable in terms of operational stability, storage stability, operating pH range etc. These encouraging observations led to the investigation of the reusability of the functionalized membrane and SLB to investigate the economic improvement of process in industries.

5.5 Reusability of the functionalized membrane and the phospholipid bilayer:

Reversibly attached phospholipid bilayer (SLB) functionalized membrane enabled reusability of the membrane matrix as well as the phospholipid bilayer. The functionalized architecture was constructed based on electrostatic interactions, which facilitate reversible attachment-detachment sequence of the functional moieties. First, the enzyme was detached keeping the functional SLB backbone intact and reusability of the functionalized membrane was demonstrated. Then, SLB was detached to obtain DMPC SUVs and the reusability of the SUVs was investigated.

5.5.1 Detachment of GOx – reusability of the SLB functionalized membrane:

To study the reusability of the functionalized biomimetic membrane, pH was manipulated to alter the reversible type of electrostatic interaction between the charged amino acid residues of the enzymes and the charged functional moieties of SLB (Figure 5.19). The pI of GOx is 4.2, hence at an operating pH of 3.5, GOx became positively charged and the electrostatic interaction with the positively charged amine groups of SLB disappeared resulting into detachment from the membrane matrix. SLB, however, remained intact under this condition. The amount of detached GOx was 92 ± 6 % of the immobilized GOx. After detaching GOx, residual activity of the biomimetic membrane was determined to be 11 ± 1 % of the initial activity. The residual activity was due to the undetached enzyme molecules still present within the functionalized matrix. The existence of the undetached enzyme molecules could be attributed to few inaccessible pockets within the functionalized architecture. When freshly attached GOx was used for detachment, activity of the detached GOx in the eluate was found to be same as the original activity in homogeneous phase. This proves that the detachment technique did not adversely affect the activity of the enzyme.

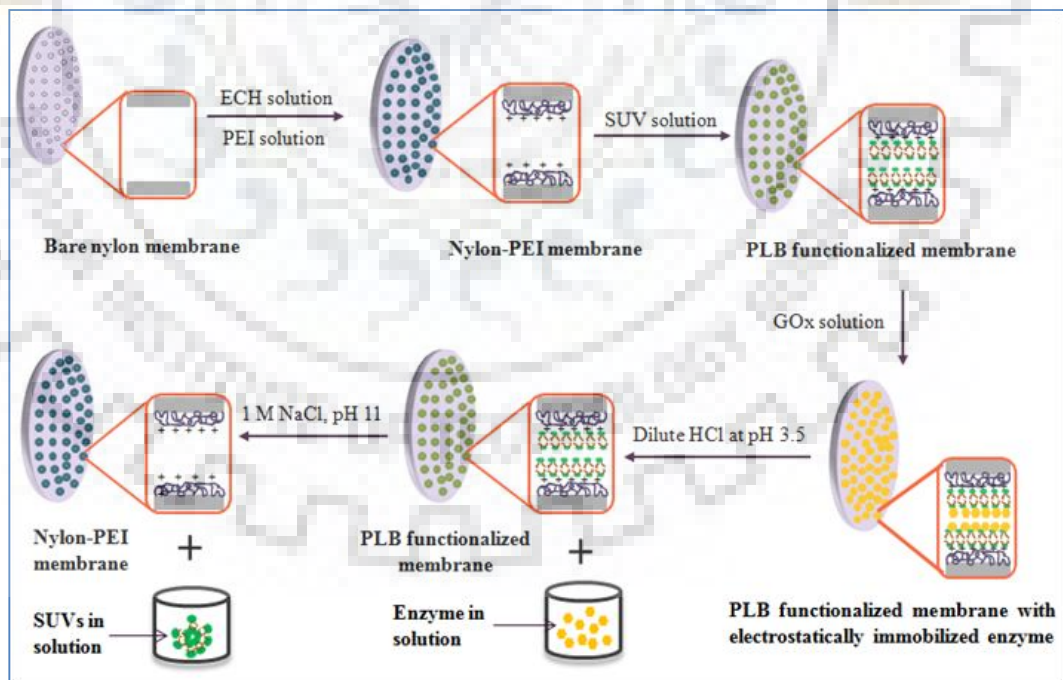


Figure 5.19. Schematic representation of formation of reversibly attached phospholipid bilayer (SLB) functionalized nylon membrane pores containing electrostatically immobilized GOx followed by sequential detachment of GOx and SLB.

To demonstrate reusability of the functionalized membrane after detachment of GOx, fresh GOx was attached to the same membrane and activity was analyzed under the same conditions as used for initial activity analysis. The activity of the fresh GOx within the reused membrane was observed to be same as the initially attached GOx (Figure 5.20). This study shows the reusability of the SLB functionalized biomimetic membrane for repeated enzymatic catalysis due to electrostatic interactions.

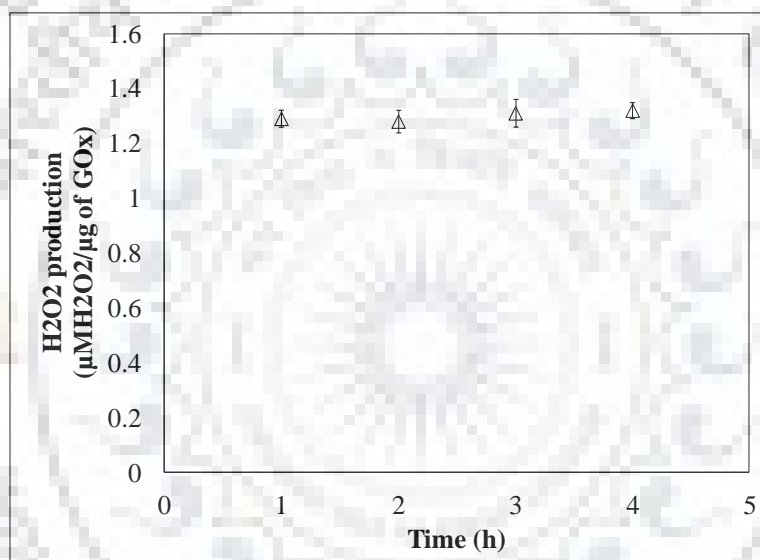


Figure 5.20. Continuous production of hydrogen peroxide by oxidation of glucose using electrostatically immobilized fresh GOx within reused membrane

5.5.3 Detachment of SLB – reusability of the phospholipid: SLB was detached with 1 M NaCl solution at pH 11. The amine groups of PEI have pK_a of around 9, hence at a pH of 11, the amine groups of PEI became deprotonated (uncharged) and the attractive interaction with the negatively charged phosphate groups of SLB disappeared (Figure 5.19). The charge shielding effect of NaCl further aided the detachment of SLB at high salt concentration. The amount of detached DMPC was 90 ± 4 % of the initially attached DMPC. To examine whether the detached phospholipid in eluate retained its structural and functional characteristics, two different strategies

were adopted – (i) Analysis by ^1H NMR spectroscopy, and (ii) Monitoring the sequential steps of formation of SLB on copper grid by TEM. To establish the structural purity of the eluted phospholipid, the stock DMPC (used for initial SLB formation) and the detached DMPC were analyzed by ^1H NMR. Comparison of the ^1H NMR spectra for the stock and the detached DMPC in Figure 5.21 revealed the structural resemblance of the samples before attachment and post-detachment. Appearance of no additional peak in the spectrum of the detached DMPC confirmed the stability of the covalently anchored PEI cushion within membrane pores.

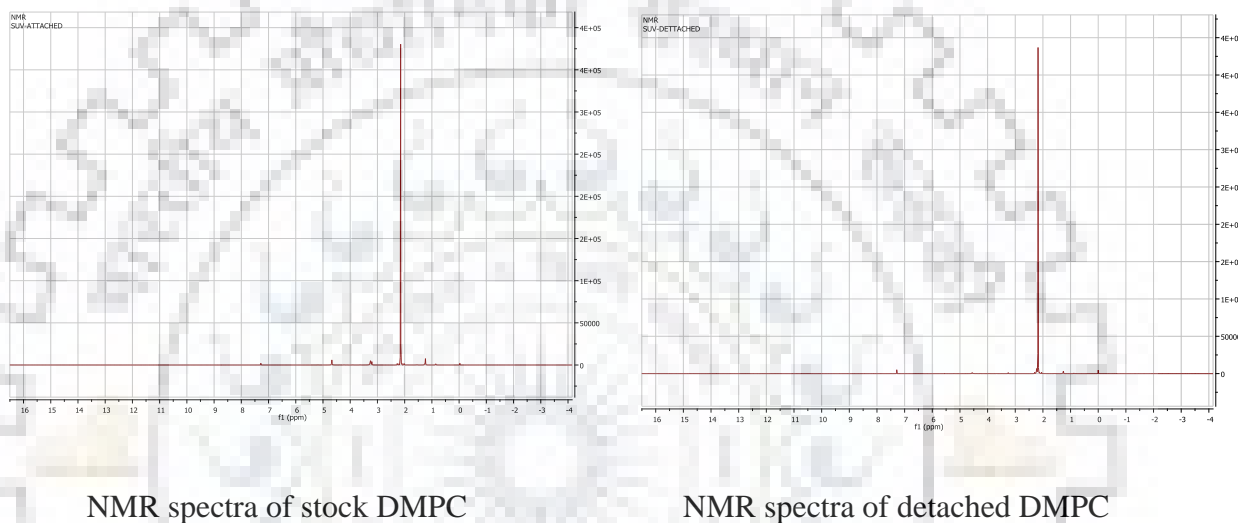


Figure 5.21 ^1H NMR spectrum of DMPC solutions at 25 °C.

SLB formation on solid surface starting from SUVs by VF technique primarily involves five major steps – (i) Approach, (ii) Fusion, (iii) Flattening, (iv) Expansion/Sliding, and (v) SLBs, as illustrated in the Introduction section. The stock and the detached DMPC solutions were spread onto TEM copper grid and different steps of SLB formation was monitored by TEM (50000x magnification). TEM micrographs for different steps are represented in Figure 5.22. The above mentioned five major steps of SLB formation are distinctly visible for both the stock and the detached DMPC solutions. This observation suggests that the functional characteristics of the detached phospholipid remained intact. To check the reusability of the detached DMPC, it was reattached within nylon-PEI membrane followed by attachment of GOx as stated earlier. The activity of GOx in presence of the reattached DMPC was observed to be identical to the activity of

GOx in presence of the freshly attached DMPC. Hence, the detached DMPC could be reused for successive cycles of membrane functionalization or could be used for other applications, thereby significantly improving the economic viability of the process.

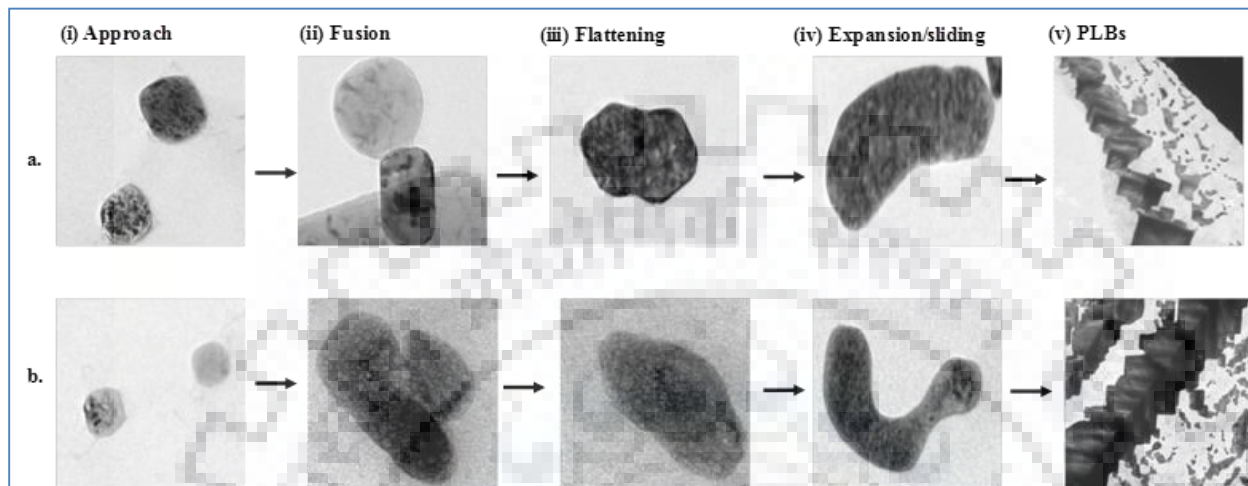


Figure 5.22. TEM micrographs for steps of SLB formation on TEM copper grid using a. stock DMPC solution before attachment, and b. detached DMPC solution.

Chapter 6: Conclusions

A novel phospholipid bilayer functionalized biomimetic membrane was developed. Phospholipid bilayer (PLB) was incorporated within the pores of the membrane. As model enzyme, glucose oxidase (GOx) was immobilized within the pores of the biomimetic membrane and immobilized enzymatic catalysis was conducted. The study was further extended for development of bienzymatic (glucose oxidase-horseradish peroxidase) and multienzymatic (glucoamylase-glucose oxidase-horseradish peroxidase) systems. Detailed investigation of the immobilized enzymatic catalysis revealed that a polymer cushion supported PLB and convective mode of flow lead to improved performance in terms of activity, stability and reusability. To the best of our knowledge, this is the first reported study on formation of phospholipid bilayer within membrane pores using reversible type of electrostatic interactions that enabled reusability of the membrane matrix and other functional components. Detailed descriptions of the concluding remarks are given below.

Novel biomimetic membrane was developed by incorporating phospholipid bilayer within nylon membrane pores. Two different functionalization approaches were used. In one approach, lipid bilayer was directly deposited within bare membrane pores (L). In another approach, prior to lipid bilayer, a polymer cushion was incorporated within membrane pores (CL). CL was found to have ~ 83 % enhanced lipid incorporation as compared to L. The study was further extended by immobilizing a model enzyme, glucose oxidase (GOx), within the pores of the functionalized membranes for enzymatic catalysis. CL was found to be superior to L both in terms of the enzyme loading (~2 times higher) and enzyme activity (~ 91 % higher). These can be correlated to the lipid bilayer formation on extended cushion of polymers within the pores of CL. CL also demonstrated superior performance over an earlier reported study on electrostatically immobilized GOx within PVDF-PAA functionalized membrane pores. This can be attributed to the native “cell membrane” ambience provided by the lipid bilayer. It was also observed that the convective mode of flow was able to achieve ~ 2 orders of magnitude higher rate of product formation than diffusive mode of flow through the same CL membrane. In comparison to free GOx, immobilized GOx within CL membrane demonstrated improved stability over a period of 28 days and enabled a broader range of operating pH (4 to 8) without substantial loss of activity. Overall, biomimetic

membrane containing polymer cushion supported phospholipid bilayer and operating under convective mode of flow exhibited important advancements in the field of immobilized enzymatic catalysis in terms of activity, stability and operating range of pH.

Further, an efficient immobilized GOx-HRP bienzymatic system was developed by electrostatically immobilizing the two enzymes within phospholipid bilayer functionalized membrane pores. Point to be noted that GOx and HRP were immobilized by utilizing negative and positive charges, respectively. Membrane functionalized with polymer cushion supported lipid bilayer (CL) was found to be superior to lipid bilayer deposited membrane (L) both in terms of enzyme loading and activity for single enzyme. Hence, CL membrane was selected for development of GOx-HRP bienzymatic system. Two different approaches were used to develop CL containing GOx-HRP bienzymatic system. In one approach, GOx and HRP enzymes were electrostatically immobilized on two separate CL membranes in stack configuration (CL-S). In another approach, both GOx and HRP enzymes were immobilized within the same CL membrane in co-immobilization configuration (CL-C). CL-C GOx-HRP bienzymatic system was associated with higher activity than CL-S system due to the proximity of the enzymes. The H₂O₂ utilization efficiency for CL-C was found to be higher than CL-S reestablishing the superiority of CL-C over CL-S. Storage stability of both CL-S and CL-C was significantly higher than the free enzymes over a period of 28 days. Operating range of pH was also observed to be broader (pH ~ 5 to 9) for both CL-S and CL-C bienzymatic system as compared to the free enzymes. One of the major conclusions of this study was that this phospholipid bilayer functionalized membrane can be implemented for the electrostatic immobilization of enzymes containing either positive or negative charge under suitable physical conditions.

CL membranes were further utilized for the development of GA-GOx-HRP based multienzymatic system. Since, CL-C was observed to be superior than CL-S during GOx-HRP bienzymatic system development, CL membrane containing immobilized GA and CL-C membrane having immobilized GOx-HRP enzymes were used in stack configuration for multienzymatic system development. Such developed multienzymatic system was observed to be efficient in terms of activity, pH activity profile and storage stability as compare to the free enzymes.

Finally, the reusability of the functionalized membrane as well as the functional components was explored by exploiting the reversible type of interactions among the constituents. Reversibility emerged due to the electrostatic attachment of the functionalized moieties. Glucose oxidase (GOx) was used as a model enzyme to study the reusability of the biomimetic membrane containing phospholipid bilayer. First, GOx was detached by a simple manipulation of operating pH keeping the PLB backbone intact. The PLB functionalized membrane was reused for further attachment of GOx. This approach could be useful to remove the deactivated enzyme and replenish the same membrane matrix with fresh enzyme. Alternatively, it can be implemented to immobilize different enzymes for different applications without changing the membrane matrix. Then, the PLB was sequentially detached using a simple technique. Characterization of the detached phospholipid confirmed retention of the original structural and functional properties as exhibited before attachment. The detached phospholipid was reattached to form PLB functionalized biomimetic membrane and demonstrated similar performance as before.

With further improvements in system design and process optimization, the proposed phospholipid bilayer functionalized biomimetic membrane containing immobilized enzyme could become a valuable tool for various industrial applications.

Abbreviations

ABTS	2,2'-Azino-bis-(3-ethylbenzothiazoline-6-sulfonic acid) diammonium salt
DMPC	1,2-dimyristoyl-sn-glycero-3-phosphocholine
ECH	Epichlorohydrin
GA	Glucoamylase
GOx	Glucose oxidase
HRP	Horseradish peroxidase
PEI	Polyethyleneimine
PLB	Phospholipid bilayer
PVDF	Polyvinylidene fluoride
SLB	Supported lipid bilayer
SUV	Small unilamellar vesicles
VF	Vesicle fusion

Chapter 7: References

- [1] S.R. and R. Gupta, Advantages of the Immobilization of Lipase on Porous Supports Over Free Enzyme, *Protein Pept. Lett.* **17** (2010) 1412–1416. doi:http://dx.doi.org/10.2174/0929866511009011412.
- [2] S. Vishwanath, D. Bhattacharyya, W. Huang, L.G. Bachas, Site-directed and random enzyme immobilization on functionalized membranes: kinetic studies and models, *J. Memb. Sci.* **108** (1995) 1–13. doi:10.1016/0376-7388(95)00135-9.
- [3] S. Datta, C. Cecil, D. Bhattacharyya, Functionalized membranes by layer-by-layer assembly of polyelectrolytes and in situ polymerization of acrylic acid for applications in enzymatic catalysis, *Ind. Eng. Chem. Res.* **47** (2008) 4586–4597. doi:10.1021/ie800142d.
- [4] Y. xiao Shen, P.O. Saboe, I.T. Sines, M. Erbakan, M. Kumar, Biomimetic membranes: A review, *J. Memb. Sci.* **454** (2014) 359–381. doi:10.1016/j.memsci.2013.12.019.
- [5] J.T. Groves, N. Ulman, P.S. Cremer, S.G. Boxer, Substrate–Membrane Interactions: Mechanisms for Imposing Patterns on a Fluid Bilayer Membrane, *Langmuir.* **14** (1998) 3347–3350. doi:10.1021/la9711701.
- [6] J.S. Hovis, S.G. Boxer, Patterning barriers to lateral diffusion in supported lipid bilayer membranes by blotting and stamping, *Langmuir.* **16** (2000) 894–897.
- [7] C.A. Naumann, O. Prucker, T. Lehmann, J. R uhe, W. Knoll, C.W. Frank, The polymer-supported phospholipid bilayer: Tethering as a new approach to substrate-membrane stabilization, *Biomacromolecules.* **3** (2002) 27–35. doi:10.1021/bm0100211.
- [8] E. Reimhult, F. H ok, B. Kasemo, Intact vesicle adsorption and supported biomembrane formation from vesicles in solution: Influence of surface chemistry, vesicle size, temperature, and osmotic pressure, *Langmuir.* **19** (2003) 1681–1691. doi:10.1021/la0263920.
- [9] R.P. Richter, R. B erat, A.R. Brisson, Formation of solid-supported lipid bilayers: An

integrated view, *Langmuir*. **22** (2006) 3497–3505. doi:10.1021/la052687c.

- [10] A. Deniaud, C. Rossi, A. Berquand, J. Homand, S. Campagna, W. Knoll, C. Brenner, J. Chopineau, Voltage-dependent anion channel transports calcium ions through biomimetic membranes, *Langmuir*. **23** (2007) 3898–3905. doi:10.1021/la063105+.
- [11] C. Rossi, J. Chopineau, Biomimetic tethered lipid membranes designed for membrane-protein interaction studies, *Eur. Biophys. J.* **36** (2007) 955–965. doi:10.1007/s00249-007-0202-y.
- [12] J. Jass, T. Tjärnhage, G. Puu, From liposomes to supported, planar bilayer structures on hydrophilic and hydrophobic surfaces: An atomic force microscopy study, *Biophys. J.* **79** (2000) 3153–3163. doi:10.1016/S0006-3495(00)76549-0.
- [13] E.T. Castellana, P.S. Cremer, Solid supported lipid bilayers: From biophysical studies to sensor design, *Surf. Sci. Rep.* **61** (2006) 429–444. doi:10.1016/j.surfrep.2006.06.001.
- [14] E. Piacentini, R. Mazzei, E. Drioli, L. Giorno, From Biological Membranes to Artificial Biomimetic Membranes and Systems, 2017. doi:10.1016/B978-0-12-409547-2.12236-X.
- [15] R. Mazzei, L. Giorno, Editorial: Bio-inspired Membranes for Separation Conversion Sensing and Bioartificial Systems, 2017. doi:10.2174/138527282117170830093919.
- [16] J.J. Ramsden, Biomimetic protein immobilization using lipid bilayers, *Biosens. Bioelectron.* **13** (1998) 593–598. doi:10.1016/S0956-5663(98)00014-1.
- [17] L. Giorno, E. Drioli, Biocatalytic membrane reactors: Applications and perspectives, *Trends Biotechnol.* **18** (2000) 339–349. doi:10.1016/S0167-7799(00)01472-4.
- [18] S. Chede, N.M. Anaya, V. Oyanedel-craver, S. Gorgannejad, T.A.L. Harris, J. Al-mallahi, M. Abu-dalo, H.A. Qdais, I.C. Escobar, Desalination using low biofouling nanocomposite membranes: From batch-scale to continuous-scale membrane fabrication, *Desalination*. (2017) 1–11. doi:10.1016/j.desal.2017.05.007.
- [19] V.S. Arijit Das, C. Das G Pugazhenth, M. Srinivas, Fouling and Cleaning Characteristics of Reverse Osmosis (RO) Membranes, *J. Chem. Eng. Process Technol.* **06** (2015) 6–11.

doi:10.4172/2157-7048.1000244.

- [20] F.Q. Mir, A. Shukla, Negative rejection of NaCl in ultrafiltration of aqueous solution of NaCl and KCl using sodalite octahydrate zeolite-clay charged ultrafiltration membrane, *Ind. Eng. Chem. Res.* **49** (2010) 6539–6546. doi:10.1021/ie901775v.
- [21] R. Mazzei, E. Drioli, L. Giorno, Enzyme membrane reactor with heterogenized β -glucosidase to obtain phytotherapeutic compound: Optimization study, *J. Memb. Sci.* **390–391** (2012) 121–129. doi:10.1016/j.memsci.2011.11.028.
- [22] M. Mondal, S. De, Characterization and antifouling properties of polyethylene glycol doped PAN–CAP blend membrane, *RSC Adv.* **5** (2015) 38948–38963. doi:10.1039/C5RA02889B.
- [23] R.S. Kumar, G. Arthanareeswaran, D. Paul, J.H. Kweon, Modification methods of polyethersulfone membranes for minimizing fouling – Review, **4** (2015) 323–337.
- [24] K. Suresh, G. Pugazhenti, Development of ceramic membranes from low-cost clays for the separation of oil-in-water emulsion, *Desalin. Water Treat.* **57** (2016) 1927–1939. doi:10.1080/19443994.2014.979445.
- [25] R.V. Kumar, A.K. Ghoshal, G. Pugazhenti, Fabrication of zirconia composite membrane by in-situ hydrothermal technique and its application in separation of methyl orange, *Ecotoxicol. Environ. Saf.* **121** (2015) 73–79. doi:10.1016/j.ecoenv.2015.05.006.
- [26] M. Kumar, M. Grzelakowski, J. Zilles, M. Clark, W. Meier, Highly permeable polymeric membranes based on the incorporation of the functional water channel protein Aquaporin Z, **104** (2007) 20719–20724.
- [27] S. Workneh, A. Shukla, Synthesis of sodalite octahydrate zeolite-clay composite membrane and its use in separation of SDS, *J. Memb. Sci.* **309** (2008) 189–195. doi:10.1016/j.memsci.2007.10.033.
- [28] A. Shukla, A. Kumar, Characterization of chemically modified zeolite-clay composite membranes using separation of trivalent cations, *Sep. Purif. Technol.* **41** (2005) 83–89. doi:10.1016/j.seppur.2004.05.001.

- [29] T. N Shah, J. C Goodwin, S. M C Ritchie, Esterification Using Polymeric Catalytic Microfiltration Membrane Functionalized by Cationic Polymerization of Styrene, 2018.
- [30] S. M. C. Ritchie, L. G. Bachas, T. Estes, S. Sikdar, D. Bhattacharyya, Surface Modification of Silica- and Cellulose-Based Microfiltration Membranes with Functional Polyamino Acids for Heavy Metal Sorption, 1999. doi:10.1021/la9814438.
- [31] J.F. Kim, J.H. Kim, Y.M. Lee, E. Drioli, Thermally Induced Phase Separation and Electrospinning Methods for Emerging Membrane Applications : *A Review*, **62** (2016) 461–490. doi:10.1002/aic.
- [32] J. Eke, P. Wagh, I.C. Escobar, Ozonation , Biofiltration and the Role of Membrane Surface Charge and Hydrophobicity in Removal and Destruction of Algal ... hydrophobicity in removal and destruction of algal toxins at basic pH values, *Sep. Purif. Technol.* **194** (2017) 56–63. doi:10.1016/j.seppur.2017.11.034.
- [33] R. Mukherjee, R. Sharma, S. De, Environmental Science Nanostructured polyaniline incorporated ultrafiltration membrane for desalination of brackish water †, *Environ. Sci. Water Res. Technol.* **1** (2015) 893–904. doi:10.1039/C5EW00163C.
- [34] A. Kumar, P. Vatsyayan, P. Goswami, S.D. Minter, Recent advances in material science for developing enzyme electrodes, *Biosensors and Bioelectronics* **24** (2009) 2313–2322. doi:10.1016/j.bios.2008.09.026.
- [35] S.R. Panda, M. Mukherjee, S. De, Journal of Water Process Engineering Preparation , characterization and humic acid removal capacity of chitosan coated iron-oxide-polyacrylonitrile mixed matrix membrane, *J. Water Process Eng.* **6** (2015) 93–104. doi:10.1016/j.jwpe.2015.03.007.
- [36] D. Bhattacharyya, J.A. Hestekin, S.M.C. Ritchie, L.G. Bachas, Functionalised membranes remove and recover dissolved heavy metals, *Membr. Technol.* 1999 (1999) 8–11.
- [37] M. Pinelo, G. Jonsson, A.S. Meyer, Membrane technology for purification of enzymatically produced oligosaccharides: Molecular and operational features affecting performance, *Sep. Purif. Technol.* **70** (2009) 1–11. doi:10.1016/j.seppur.2009.08.010.

- [38] P. Jochems, Y. Satyawali, L. Diels, W. Dejonghe, Enzyme immobilization on/in polymeric membranes: status, challenges and perspectives in biocatalytic membrane reactors (BMRs), *Green Chem.* **13** (2011) 1609. doi:10.1039/c1gc15178a.
- [39] M. Kumar, Y. Shen, P.O. Saboe, E.M. V Hoek, V. V Tarabara, Biological and Biomimetic Membranes, in: *Encycl. Membr. Sci. Technol.*, 2013: pp. 1–37. doi:10.1002/9781118522318.emst051.
- [40] E.T. Castellana, P.S. Cremer, Solid supported lipid bilayers: From biophysical studies to sensor design, *Surf. Sci. Rep.* **61** (2006) 429–444.
- [41] M.-P. Mingeot-Leclercq, M. Deleu, R. Brasseur, Y.F. Dufrêne, Atomic force microscopy of supported lipid bilayers, *Nat. Protoc.* **3** (2008) 1654–1659. doi:10.1038/nprot.2008.149.
- [42] C.A. Keller, K. Glasmästar, V.P. Zhdanov, B. Kasemo, Formation of Supported Membranes from Vesicles, *Phys. Rev. Lett.* **84** (2000) 5443–5446. doi:10.1103/PhysRevLett.84.5443.
- [43] J.A. Jackman, W. Knoll, N.J. Cho, Biotechnology applications of tethered lipid bilayer membranes, *Materials (Basel)*. **5** (2012) 2637–2657. doi:10.3390/ma5122637.
- [44] M. Tanaka, E. Sackmann, Polymer-supported membranes as models of the cell surface, *Nature*. **437** (2005) 656–663. doi:10.1038/nature04164.
- [45] V. Atanasov, N. Knorr, R.S. Duran, S. Ingebrandt, A. Offenhäusser, W. Knoll, I. Köper, Membrane on a Chip: A Functional Tethered Lipid Bilayer Membrane on Silicon Oxide Surfaces, *Biophys. J.* **89** (2005) 1780–1788. doi:10.1529/biophysj.105.061374.
- [46] C. Rossi, J. Homand, C. Bauche, H. Hamdi, D. Ladant, J. Chopineau, Differential Mechanisms for Calcium-Dependent Protein/Membrane Association as Evidenced from SPR-Binding Studies on Supported Biomimetic Membranes, *Biochemistry*. **42** (2003) 15273–15283. doi:10.1021/bi035336a.
- [47] C. Ellis, The state of GPCR research in 2004, *Nat. Rev. Drug Discov.* **3** (2004) 577–626.
- [48] C.-J. Huang, A. Harootunian, M.P. Maher, C. Quan, C.D. Raj, K. McCormack, R. Numann,

- P.A. Negulescu, J.E. González, Characterization of voltage-gated sodium-channel blockers by electrical stimulation and fluorescence detection of membrane potential, *Nat. Biotechnol.* **24** (2006) 439–446.
- [49] R.A. Lerner, Manufacturing immunity to disease in a test tube: the magic bullet realized, *Angew. Chemie Int. Ed.* **45** (2006) 8106–8125.
- [50] P. Holliger, P.J. Hudson, Engineered antibody fragments and the rise of single domains, *Nat. Biotechnol.* **23** (2005) 1126–1136.
- [51] L.L. Kiessling, J.E. Gestwicki, L.E. Strong, Synthetic multivalent ligands in the exploration of cell-surface interactions, *Curr. Opin. Chem. Biol.* **4** (2000) 696–703.
- [52] M. Ferrari, Cancer nanotechnology: opportunities and challenges, *Nat. Rev. Cancer.* **5** (2005) 161–171.
- [53] J. Rädler, E. Sackmann, Functionalization of solids by ultrathin soft polymer films and polymer/lipid film composites: modeling of cell surfaces and cell recognition processes, *Curr. Opin. Solid State Mater. Sci.* **2** (1997) 330–336.
- [54] E. Sackmann, Supported Membrane: Scientific and Practical Applications, *Science* **271** (1996) 43.
- [55] T.J. Crites, M. Maddox, K. Padhan, J. Muller, C. Eigsti, R. Varma, Supported Lipid Bilayer Technology for the Study of Cellular Interfaces., 2015. doi:10.1002/0471143030.cb2405s68.
- [56] P. Binod, P. Palkhiwala, R. Gaikawai, K. Madhavan Nampoothiri, A. Duggal, K. Dey, A. Pandey, Industrial enzymes - Present status and future perspectives for india, *J. Sci. Ind. Res. (India)*. **72** (2013) 271–286.
- [57] P. Jönsson, M.P. Jonsson, J.O. Tegenfeldt, F. Höök, A method improving the accuracy of fluorescence recovery after photobleaching analysis., *Biophys. J.* **95** (2008) 5334–5348. doi:10.1529/biophysj.108.134874.
- [58] P. Alessio, C.S. Martin, J.A. De Saja, M.L. Rodriguez-Mendez, Mimetic biosensors

- composed by layer-by-layer films of phospholipid, phthalocyanine and silver nanoparticles to polyphenol detection, *Sensors Actuators, B Chem.* **233** (2016) 654–666. doi:10.1016/j.snb.2016.04.139.
- [59] P.R. Cullis, M.J. Hope, Chapter 1 Physical properties and functional roles of lipids in membranes, *New Compr Biochem.* **20** (1991) 1–41. <http://www.sciencedirect.com/science/article/pii/S0167730608603294>.
- [60] K.L. Lewis, L.S.L. Su, F.M. Hawkrigde, K.R. Ward, M.C. Rhoten, Immobilization of cytochrome c oxidase into electrode-supported lipid bilayer membranes for in vitro cytochrome c sensing, *IEEE Sens. J.* **6** (2006) 420–427. doi:10.1109/JSEN.2006.870137.
- [61] H. Mao, T. Yang, P.S. Cremer, Design and characterization of immobilized enzymes in microfluidic systems, *Anal. Chem.* **74** (2002) 379–385. doi:10.1021/ac010822u.
- [62] Q. Ji, B. Wang, J. Tan, L. Zhu, L. Li, Immobilized multienzymatic systems for catalysis of cascade reactions, *Process Biochem.* **51** (2016) 1193–1203. doi:10.1016/j.procbio.2016.06.004.
- [63] F. Zhao, H. Li, Y. Jiang, X. Wang, X. Mu, Co-immobilization of multi-enzyme on control-reduced graphene oxide by non-covalent bonds: an artificial biocatalytic system for the one-pot production of gluconic acid from starch, *Green Chem.* **16** (2014) 2558. doi:10.1039/c3gc42545b.
- [64] T.C. Logan, D.S. Clark, T.B. Stachowiak, F. Svec, J.M.J. Fréchet, Photopatterning enzymes on polymer monoliths in microfluidic devices for steady-state kinetic analysis and spatially separated multi-enzyme reactions, *Anal. Chem.* **79** (2007) 6592–6598. doi:10.1021/ac070705k.
- [65] J. Sun, J. Ge, W. Liu, M. Lan, H. Zhang, P. Wang, Y. Wang, Z. Niu, Multi-enzyme co-embedded organic–inorganic hybrid nanoflowers: synthesis and application as a colorimetric sensor, *Nanoscale.* **6** (2014) 255–262. doi:10.1039/C3NR04425D.
- [66] L. Betancor, C. Berne, H.R. Luckarift, J.C. Spain, Coimmobilization of a redox enzyme and a cofactor regeneration system., *Chem. Commun. (Camb).* **298** (2006) 3640–3642.

doi:10.1039/b604689d.

- [67] L. Betancor, H.R. Luckarift, Co-immobilized coupled enzyme systems in biotechnology, *Biotechnol. Genet. Eng. Rev.* **27** (2010) 95–114. doi:10.1080/02648725.2010.10648146.
- [68] A.A. Homaei, R. Sariri, F. Vianello, R. Stevanato, Enzyme immobilization: An update, *J. Chem. Biol.* **6** (2013) 185–205. doi:10.1007/s12154-013-0102-9.
- [69] R. Cazelles, J. Drone, F. Fajula, O. Ersen, S. Moldovan, A. Galarneau, Reduction of CO₂ to methanol by a polyenzymatic system encapsulated in phospholipids-silica nanocapsules, *New J. Chem.* **37** (2013) 3721–3730. doi:10.1039/c3nj00688c.
- [70] J. Luo, A.S. Meyer, R. V. Mateiu, M. Pinelo, Cascade catalysis in membranes with enzyme immobilization for multi-enzymatic conversion of CO₂ to methanol, *N. Biotechnol.* **32** (2015) 319–327. doi:10.1016/j.nbt.2015.02.006.
- [71] J.L. Lopez, S.L. Matson, A multiphase/extractive enzyme membrane reactor for production of diltiazem chiral intermediate, *J. Memb. Sci.* **125** (1997) 189–211. doi:10.1016/S0376-7388(96)00292-X.
- [72] D.F. Hochstrasser, Toward a Clinical Molecular Scanner for Proteome Research: Parallel Protein Chemical Processing before and during Western Blot, *Anal. Chem.* **71** (1999) 4800–4807. doi:10.1021/ac990448m.
- [73] L. Ying, E.T. Kang, K.G. Neoh, Covalent immobilization of glucose oxidase on microporous membranes prepared from poly(vinylidene fluoride) with grafted poly(acrylic acid) side chains, *J. Memb. Sci.* **208** (2002) 361–374. doi:10.1016/S0376-7388(02)00325-3.
- [74] S. Rauf, A. Ihsan, K. Akhtar, M.A. Ghauri, M. Rahman, M.A. Anwar, A.M. Khalid, Glucose oxidase immobilization on a novel cellulose acetate- polymethylmethacrylate membrane, *J. Biotechnol.* **121** (2006) 351–360. doi:10.1016/j.jbiotec.2005.08.019.
- [75] N. Hilal, V. Kochkodan, R. Nigmatullin, V. Goncharuk, L. Al-Khatib, Lipase-immobilized biocatalytic membranes for enzymatic esterification: Comparison of various approaches to membrane preparation, *J. Memb. Sci.* **268** (2006) 198–207.

doi:10.1016/j.memsci.2005.06.039.

- [76] D. Bhattacharyya, A.D.A. Butterfield, *New insights into membrane science and technology: polymeric and biofunctional membranes*, Elsevier, 2003.
- [77] C. Mateo, J.M. Palomo, G. Fernandez-Lorente, J.M. Guisan, R. Fernandez-Lafuente, Improvement of enzyme activity, stability and selectivity via immobilization techniques, *Enzyme Microb. Technol.* **40** (2007) 1451–1463. doi:10.1016/j.enzmictec.2007.01.018.
- [78] S.R. Tabaei, F. Guo, F.U. Rutaganira, S. Vafaei, I. Choong, K.M. Shokat, J.S. Glenn, N.J. Cho, Multistep Compositional Remodeling of Supported Lipid Membranes by Interfacially Active Phosphatidylinositol Kinases, *Anal. Chem.* **88** (2016) 5042–5045. doi:10.1021/acs.analchem.6b01293.
- [79] L.T. Nguyen, K.L. Yang, Combined cross-linked enzyme aggregates of horseradish peroxidase and glucose oxidase for catalyzing cascade chemical reactions, *Enzyme Microb. Technol.* **100** (2017) 52–59. doi:10.1016/j.enzmictec.2017.02.007.
- [80] N.J. Kruger, The Bradford Method for Protein Quantitation, in: *Basic Protein Pept. Protoc.*, 1994: pp. 9–16. doi:10.1385/0-89603-268-X:9.
- [81] G.L. Miller, Use of Dinitrosalicylic Acid Reagent for Determination of Reducing Sugar, *Anal. Chem.* **31** (1959) 426–428. doi:10.1021/ac60147a030.
- [82] G. Eisenberg, Colorimetric Determination of Hydrogen Peroxide, *Ind. Eng. Chem. Anal. Ed.* **15** (1943) 327–328. doi:10.1021/i560117a011.
- [83] J.-B. du Prel, G. Hommel, B. Röhrig, M. Blettner, Confidence interval or p-value?: part 4 of a series on evaluation of scientific publications., *Dtsch. Arztebl. Int.* **106** (2009) 335–9. doi:10.3238/arztebl.2009.0335.
- [84] J.Y. Wong, J. Majewski, M. Seitz, C.K. Park, J.N. Israelachvili, G.S. Smith, Polymer-cushioned bilayers. I. A structural study of various preparation methods using neutron reflectometry, *Biophys. J.* **77** (1999) 1445–1457. doi:10.1016/S0006-3495(99)76992-4.
- [85] P. Greenspan, E.P. Mayer, S.D. Fowler, Nile red: a selective fluorescent stain for

intracellular lipid droplets, *J. Cell Biol.* **100** (1985) 965–973., *J. Cell Biol.* 100 (1985) 965–973. doi:10.1083/jcb.100.3.965.

- [86] A. Sharma, U.S. Sharma, Liposomes in drug delivery: Progress and limitations, *Int. J. Pharm.* **154** (1997) 123–140. doi:10.1016/S0378-5173(97)00135-X.
- [87] D.A. Butterfield, An overview of biofunctional membranes for tunable separations, metal-ion capture, and enzyme catalysis based on research from the laboratories of Allan Butterfield and Dibakar Bhattacharyya, *Sep. Sci. Technol.* **43** (2008) 3942–3954. doi:10.1080/01496390802414551.
- [88] B.M. Brena, F. Batista-Viera, Immobilization of enzymes: a literature survey, *Immobil. Enzym. Cells.* (2006) 15–30.
- [89] P.V. Danckwerts, Continuous flow systems, *Chem. Eng. Sci.* **2** (1953) 1–13. doi:10.1016/0009-2509(53)80001-1.
- [90] T. Chen, H. Weng, A method for the determinations of the activity and optimal pH of glucose oxidase in an unbuffered solution, *Biotechnol. Bioeng.* **28** (1986) 107–109.
- [91] D.K. Ahuja, D.K. Ahuja, Degradation of toxic chloroethylenes and chloroaromatics by vitamin B12-based reductive dechlorination and by hydroxyl radical-based oxidative dechlorination reactions, Ph.D. Thesis, University of Kentucky, Lexington, KY, 2006.
- [92] G.G. Guilbault, G.J. Lubrano, An enzyme electrode for the amperometric determination of glucose, *Anal. Chim. Acta.* **64** (1973) 439–455.
- [93] R. Wilson, A.P.F. Turner, Glucose oxidase: an ideal enzyme, *Biosens. Bioelectron.* **7** (1992) 165–185. doi:10.1016/0956-5663(92)87013-F.
- [94] L. Doretto, D. Ferrara, S. Lora, Enzyme-entrapping membranes for biosensors obtained by radiation-induced polymerization, *Biosens. Bioelectron.* **8** (1993) 443–450.
- [95] Y. Arica, V.N. Hasirci, Immobilization of glucose oxidase in poly(2-hydroxyethyl methacrylate) membranes, *Biomaterials.* **8** (1987) 489–495. doi:10.1016/0142-9612(87)90087-1.

- [96] C. Galiatsatos, Y. Ikariyama, J.E. Mark, W.R. Heineman, Immobilization of glucose oxidase in a poly [vinyl alcohol] matrix on platinized graphite electrodes by gamma-irradiation, *Biosens. Bioelectron.* **5** (1990) 47–61.
- [97] M. Portaccio, M. El-Masry, N. Rossi Diano, A. De Maio, V. Grano, M. Lepore, P. Travascio, U. Bencivenga, N. Pagliuca, D.G. Mita, An amperometric sensor employing glucose oxidase immobilized on nylon membranes with different pore diameter and grafted with different monomers, *J. Mol. Catal. B Enzym.* **18** (2002) 49–67. doi:10.1016/S1381-1177(02)00058-9.
- [98] G. Ozyilmaz, S.S. Tukul, O. Alptekin, Activity and storage stability of immobilized glucose oxidase onto magnesium silicate, *J. Mol. Catal. B Enzym.* **35** (2005) 154–160. doi:10.1016/j.molcatb.2005.07.001.
- [99] B.F.Y. Yon-Hin, T. Crompton, C.R. Lowe, M. Smolander, Covalent Electropolymerization of Glucose Oxidase in Polypyrrole. Evaluation of Methods of Pyrrole Attachment to Glucose Oxidase on the Performance of Electropolymerized Glucose Sensors, *Anal. Chem.* **65** (1993) 2067–2071. doi:10.1021/ac00063a022.
- [100] N.C. Veitch, Horseradish peroxidase: A modern view of a classic enzyme, *Phytochemistry.* **65** (2004) 249–259. doi:10.1016/j.phytochem.2003.10.022.
- [101] A. Kumari, S. Datta, Phospholipid bilayer functionalized membrane pores for enhanced efficiency of immobilized glucose oxidase enzyme, *J. Memb. Sci.* **539** (2017) 43–51. doi:10.1016/j.memsci.2017.05.060.
- [102] B.R.E. Childs, W.G. Bardsley, The Steady-State Kinetics of Peroxidase with 2,2'-Azino-di-(3-ethylbenzthiazoline- 6-sulphonic acid) as Chromogen, *Biochem. J.* **145** (1975) 93–103. doi:10.1042/bj1450093.
- [103] H. Gustafsson, A. Kuchler, K. Holmberg, P. Walde, Co-immobilization of enzymes with the help of a dendronized polymer and mesoporous silica nanoparticles, *J. Mater. Chem. B.* **3** (2015) 6174–6184. doi:10.1039/C5TB00543D.
- [104] P. Pescador, I. Katakis, J.L. Toca-Herrera, E. Donath, Efficiency of a bienzyme sequential

- reaction system immobilized on polyelectrolyte multilayer-coated colloids, *Langmuir*. **24** (2008) 14108–14114. doi:10.1021/la8027435.
- [105] R.K. Sharma, S. Das, A. Maitra, Enzymes in the cavity of hollow silica nanoparticles, *J. Colloid Interface Sci.* **284** (2005) 358–361. doi:10.1016/j.jcis.2004.10.006.
- [106] B.C. Lai Truong Phuoc, Paco Laveille, Françoise Chamouleau, Gilbert Renard, Jullien Drone, François Fajula and Anne Galarneau*, Phospholipid-templated silica nanocapsules as efficient polyenzymatic biocatalysts, *Dalton Trans.* **39** (2010) 8511–8520. doi:10.1039/c001226b.
- [107] A. Dwevedi, Enzyme immobilization: Advances in industry, agriculture, medicine, and the environment, *Enzym. Immobil. Adv. Ind. Agric. Med. Environ.* (2016) 1–132. doi:10.1007/978-3-319-41418-8.
- [108] E. Ricca, B. Brucher, J.H. Schrittwieser, Multi-enzymatic cascade reactions: Overview and perspectives, *Adv. Synth. Catal.* **353** (2011) 2239–2262. doi:10.1002/adsc.201100256.
- [109] S.R. Lewis, S. Datta, M. Gui, E.L. Coker, F.E. Huggins, S. Daunert, L. Bachas, D. Bhattacharyya, Reactive nanostructured membranes for water purification, *Proc. Natl. Acad. Sci.* **108** (2011) 8577–8582. doi:10.1073/pnas.1101144108.
- [110] M. Salamończyk, N. Vaupotič, D. Pocięcha, C. Wang, C. Zhu, E. Gorecka, Structure of nanoscale-pitch helical phases: blue phase and twist-bend nematic phase resolved by resonant soft X-ray scattering, (2017). doi:10.1039/x0xx00000x.
- [111] H.H. Hyun, J.G. Zeikus, General biochemical characterization of thermostable pullulanase and glucoamylase from *Clostridium thermohydrosulfuricum*, *Appl. Environ. Microbiol.* **49** (1985) 1168–1173.